



HAL
open science

Eocene pre- and syn-obduction tectonics in New Caledonia (Southwest Pacific), a case for oblique subduction, transcurrent tectonics and oroclinal bending; structural and paleomagnetic evidence

Dominique Cluzel, Iseppi Marion, Yan Chen

► To cite this version:

Dominique Cluzel, Iseppi Marion, Yan Chen. Eocene pre- and syn-obduction tectonics in New Caledonia (Southwest Pacific), a case for oblique subduction, transcurrent tectonics and oroclinal bending; structural and paleomagnetic evidence. *Tectonophysics*, 2021, 811, pp.228875. 10.1016/j.tecto.2021.228875 . insu-03207625

HAL Id: insu-03207625

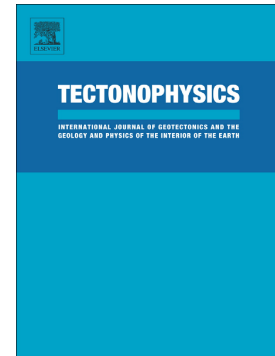
<https://insu.hal.science/insu-03207625v1>

Submitted on 26 Apr 2021

HAL is a multi-disciplinary open access archive for the deposit and dissemination of scientific research documents, whether they are published or not. The documents may come from teaching and research institutions in France or abroad, or from public or private research centers.

L'archive ouverte pluridisciplinaire **HAL**, est destinée au dépôt et à la diffusion de documents scientifiques de niveau recherche, publiés ou non, émanant des établissements d'enseignement et de recherche français ou étrangers, des laboratoires publics ou privés.

Eocene pre- and syn-obduction tectonics in New Caledonia (Southwest Pacific), a case for oblique subduction, transcurrent tectonics and oroclinal bending; structural and paleomagnetic evidence



Cluzel Dominique, Iseppi Marion, Chen Yan

PII: S0040-1951(21)00159-1

DOI: <https://doi.org/10.1016/j.tecto.2021.228875>

Reference: TECTO 228875

To appear in: *Tectonophysics*

Received date: 29 September 2020

Revised date: 8 April 2021

Accepted date: 12 April 2021

Please cite this article as: C. Dominique, I. Marion and C. Yan, Eocene pre- and syn-obduction tectonics in New Caledonia (Southwest Pacific), a case for oblique subduction, transcurrent tectonics and oroclinal bending; structural and paleomagnetic evidence, *Tectonophysics* (2021), <https://doi.org/10.1016/j.tecto.2021.228875>

This is a PDF file of an article that has undergone enhancements after acceptance, such as the addition of a cover page and metadata, and formatting for readability, but it is not yet the definitive version of record. This version will undergo additional copyediting, typesetting and review before it is published in its final form, but we are providing this version to give early visibility of the article. Please note that, during the production process, errors may be discovered which could affect the content, and all legal disclaimers that apply to the journal pertain.

Eocene pre- and syn-obduction tectonics in New Caledonia (Southwest Pacific), a case for oblique subduction, transcurrent tectonics and oroclinal bending; structural and paleomagnetic evidence.

Cluzel Dominique^{1*}, Iseppi Marion¹ and Chen Yan²

¹ Université de la Nouvelle-Calédonie, Institut des Sciences Exactes et Appliquées (EA 7484), Avenue James Cook, 98850 Nouméa, New Caledonia

² Université d'Orléans, CNRS, BRGM, ISTO, UMR 7327, F-45071, Orléans, France

* corresponding author, dominique.cluzel@unc.nc

Abstract

The structural analysis of the metamorphic belt and allochthonous terranes, which represent the lower and upper plates of the Eocene subduction/obduction complex of New Caledonia respectively, unravels a multi-step evolution. At subduction inception, the originally N-S trending northern Norfolk/New Caledonia Ridge was moving northward as recorded by sheared lower Eocene dykes of the Peridotite Nappe. Fast exhumation of the fore-arc mantle in transtensional conditions was recorded by the injection of fore-arc magmas through fast-cooling peridotites, followed by the occurrence of antigorite- and tremolite-bearing crack seals in small-scale transcurrent or oblique-slip faults. Meanwhile, slices of the oceanic crust of the lower plate were scrapped off and accumulated in the fore-arc region while some elements were dragged down into the subduction zone and contributed to the formation of eclogite facies mélange. When the tip of the New Caledonia Ridge reached the trench, it progressively jammed the subduction. Meanwhile, the oblique slip and coeval rotation of the arc due to the opening of the north Loyalty back-arc basin provoked the dextral transcurrent folding of already accreted ocean crust slices and metamorphic units on the course of exhumation. Bulk counterclockwise rotation of $56^{\circ} \pm 5^{\circ}$ was recorded in the foreland basin by paleomagnetic data of sediments from the 45-35 Ma time interval. The final obduction of fore-arc peridotites occurred with top-to-the-SW kinematics when the island had already reached its present orientation.

Keywords

Oblique subduction, fault analysis, supra-subduction dykes, transcurrent folding, paleomagnetism, oroclinal bending.

1. Introduction

The current model of Eocene tectonics in New Caledonia, which postulates northeast-dipping pre-obduction subduction on the basis of structural, metamorphic and paleogeographic evidence is generally accepted (Aitchison et al., 1995; Carson et al., 1999; Clarke et al., 1997; Cluzel et al., 2001; Fitzherbert et al., 2003; Maurizot and Cluzel, 2014; Maurizot et al., 2020c; Spandler et al., 2003, 2004; Vitale Brovarone and Agard, 2003; Vitale Brovarone et al., 2017) and inferred by mantle structure (Schellart and Spakman, 2012; Van de Lagemaat et al., 2018) and plate tectonics reconstructions as well (Schellart et al., 2006; Whattam, 2008). However, due to the relatively small amplitude of the displacement, the kinematics of pre-obduction subduction is only roughly constrained by on land paleomagnetic data (Ali and Aitchison, 2000, 2002; Dallanave et al., 2020; this study) and is therefore mainly based on structural evidence. Some features of the Eocene high pressure-low temperature (HP-LT) metamorphic belt, which relate to the lower plate of the obduction-subduction system, have not yet been considered in this regard although they have long been known (Briggs et al., 1978; Lillie and Brothers, 1970; Maurizot et al., 1989; Maurizot and Vendé-Leclerc, 2009). In obducted peridotites, which represent the upper plate of the subduction-obduction system, pre-, syn- and post-obduction brittle or semi-brittle tectonic events are overprinted and may lead to confusion because they seem difficult to unmix. Therefore, except for tectonic features of the serpentinite sole directly and obviously related to obduction (e.g., Gautier et al., 2016; Quesnel et al., 2016), a structural analysis based on accurately discriminated tectonic features is needed. Discrimination is possible on the basis of the formation depth (temperature) and nature of associated minerals. For example, the occurrence of supergene minerals in crack seals (silica, garnierite, etc.) allows the recognition of recent, shallow and dominantly gravity-driven tectonic events (Iseppi et al., 2018). While ductile deformation in peridotites and associated magmatic rocks may be attributed to deep-seated mantle tectonics. In this article, the term “obduction” strictly means “overthrusting of ocean-type lithosphere elements upon continental crust” and only relates to the tectonic events involved in the final tectonic emplacement of New Caledonia Ophiolite, hereafter referred to as Peridotite Nappe (Avias, 1967). This study based on the analysis of geological maps (online geological map of New Caledonia, DIMENC, <https://georep.nc/explorateur-cartographique>), field structural analysis and paleomagnetic data, aims at identifying pre-obduction tectonic events to constrain the kinematics of Eocene subduction. For that end, analyses of existing geological maps and field surveys have been conducted in the Eocene HP-LT metamorphic belt, and in the allochthonous Poya Terrane and Peridotite Nappe.

2. Geologic setting

New Caledonia is an elongate island (400km x 45km) at the emerged northern tip of the Norfolk/New Caledonia Ridge, a narrow ribbon of continental nature, which forms the northern part of a continent-size largely submarine area of thinned continental crust referred to as Zealandia (Luyendyk, 1995; Mortimer et al., 2017). Zealandia was originally connected to Gondwana (Australia and Antarctica) and rifted during the Late Cretaceous (Uruski and Wood, 1991).

The Norfolk Ridge is bounded on both sides by deep-water basins, New Caledonia Basin to the southwest and Loyalty Basin to the northeast (Figure 1). The boundary between the Norfolk/New Caledonia Ridge and New Caledonia Basin is underlined by a strong asymmetrical negative gravity anomaly (Collot et al., 1987; Van de Beuque, 1999) which continues northward along the hook-shaped D'Entrecasteaux Zone and disappears southward at ca 23°S. In the New Caledonia Basin the gravity anomaly is due to the thick sedimentary infill onlapping a northeast-dipping Eocene seismic reflector (Collot et al., 2008). The New Caledonia Basin has an oceanic basement with a horizontal Moho to the south of 23°S and a thinned continental basement with a northeast-dipping Moho in the northern part (Klingerhoffer et al., 2007) where it is in contact with the continental Lord Howe Rise through the Fairway Ridge. The Loyalty Basin is asymmetrical as well and its oceanic basement dips to the northeast towards the Loyalty Ridge (Bicouin and Récy, 1982). The boundary between New Caledonia Island and the Loyalty Basin is rectilinear over more than 500 km and associated with a strong positive gravimetric anomaly beneath the northeastern lagoon, which denotes the occurrence of dense mantle rocks near the surface. This linear feature represents the steeply dipping root of the ultramafic New Caledonia Ophiolite (Collot et al., 1987) referred to as Peridotite Nappe (Avias, 1967).

The geology of New Caledonia consists of: (1) pre-Late Cretaceous arc-derived basement terranes in relation to the Southeast Gondwana active margin (Meffre, 1995; Maurizot et al., 2020a) and Late Cretaceous to Eocene sedimentary cover (Maurizot et al., 2020b); (2) Eocene high pressure-low temperature metamorphic belt, which crops out in the northern part of the island (Maurizot et al., 2020c); and (3) two large allochthonous terranes: the mafic Poya Terrane emplaced in mid-Eocene time and the ultramafic Peridotite Nappe obducted at the Eocene/Oligocene boundary, which together represent almost one half of island's surface (Fig. 1a) (Cluzel et al., 2012a; Maurizot et al., 2020c).

Fig. 1 Geological sketch map of New Caledonia

The Peridotite Nappe (Avias, 1967) formed when the Loyalty Basin lithosphere was thrust upon the New Caledonia Ridge (Collot et al., 1987) when the latter reached the Loyalty subduction zone (Aitchison et al., 1995; Cluzel et al., 2001, 2017). It originally covered most of the island and extends further south on the submarine Norfolk Ridge (Patriat et al., 2018). Inception of the intra-oceanic subduction that finally led to obduction was recorded by the mafic metamorphic sole, dated at *ca* 56 Ma ($^{40}\text{Ar}/^{39}\text{Ar}$ on hornblende and U-Pb on zircon overgrowths) (Cluzel et al., 2012b). The high temperature-low pressure thermal gradient (*ca.* 60°C/km) recorded by the granulite-facies metamorphic sole suggests that subduction started near a spreading ridge. Therefore, the involved lithosphere was buoyant and the subduction zone was shallow-dipping at start. Such a tectonic regime generated strong frictional forces at the plates interface (Espert et al., 2008; Gutscher et al., 2000) until older and colder parts of the lower plate reached the subduction zone and developed high pressure-low temperature metamorphism. Remarkably, there is no evidence for normal (MOR-type) oceanic crust to exist on top of the ultramafic rocks. The strongly depleted harzburgites and dunites of the Peridotite Nappe are directly overlain by km-scale mafic-ultramafic cumulate lenses; which consist of layered dunites, pyroxenites, wehrlites, websterites and gabbro (enstatite gabbro) from the base upwards.

The Poya Terrane (or Poya Nappe) (Cluzel et al., 1997; 2001) consists of a principal unit 10 to 20 km wide, which crops out over 160 km along the west coast of the island. Smaller km-sized lenses appear beneath the Peridotite Nappe on the Massif du Sud, the northernmost massifs and along the east coast. It is composed of tectonically sliced and duplicated uppermost oceanic crust rocks and passive margin turbidites intruded by lowermost Eocene dolerite sills (Cluzel et al., 2017).

The Eocene HP-LT metamorphic belt extends over *ca* 200 km along the northeastern coast of the island, from the northern tip of the island to Houaïlou (Figure 1). It consists of two terranes: the Diahot-Panié Terrane, a dominantly metasedimentary unit, and the Pouébo Terrane, a mafic-ultramafic melange. The Diahot-Panié Terrane is principally composed of Late Cretaceous-Eocene meta-sediments and meta-volcanic rocks and volumetrically minor pre-Late Cretaceous meta-volcaniclastic rocks. The Pouébo Terrane is an eclogite-facies melange formed of cm- to km-size blocks enclosed in a meta-serpentinite matrix. Slices of lower grade mélangé squeezed within the Diahot-Panié Terrane are referred to as Intermediate Melange (Cluzel, 2020). Components of the Pouébo Terrane and Intermediate Mélangé come from the lower plate (Poya Terrane, Late Cretaceous-Paleocene metasediments) and to a lesser extent from the upper plate (serpentinite matrix, lowermost Eocene (55 Ma) fore-arc basin components: andesite pillow lavas and diorite dykes, and lower Eocene supra-subduction dykes) (Cluzel, 2020).

The post-Early Cretaceous geological evolution may be summarized as follows:

- The rifting period (Late Cretaceous) is represented in the sedimentary cover of the Norfolk Ridge by coal-bearing shallow water marine sedimentation and moderate volcanic activity. Coeval coarse- to medium grain turbidites and black shales of the Diahot-Panié Terrane were accumulated in deep- water half-grabens, while distal passive margin turbidites characterize the Kone Facies (KF, Poya Terrane). Marginal rifting is generally attributed to the eastward rollback of the Pacific slab (e.g., Schellart et al., 2006), although no trace of a Late Cretaceous volcanic arc has been hitherto discovered (Cluzel and Meffre, 2018);
- The post-rift (oceanization) period was recorded by uppermost Cretaceous to mid-Eocene fining upward sequence, which recorded thermal subsidence while marginal basins opened on both sides of the Norfolk Ridge;
- A new northeast-dipping subduction started to the north of New Caledonia at the end of the Paleocene (> 56 Ma) (Cluzel et al., 2012b), it consumed most of the South Loyalty Basin located to the east of Norfolk Ridge (Cluzel et al., 2001).
- From the mid-Eocene (*ca* 47 Ma – 45 Ma) (Dallanave et al., 2018, 2020) to the late Eocene (*ca* 34 Ma); (Cluzel et al., 1998) increasing instability in the continental lower plate (the northern Norfolk Ridge) was recorded by input of ferruginous argillite into the carbonate sedimentation, then occurrence of intraformational breccia overlain by 3-5 km thick upward coarsening turbidites. The latter accumulated in southeast-propagating foreland basin fed by parautochthonous imbricate thrusts (Montagne Blanches Nappe), (Maurizot, 2011) and from *ca* 40-38 Ma by the Poya Terrane (Maurizot & Cluzel, 2014; Maurizot et al., 2020b).
- At the end of the Late Eocene (<34 Ma), when the tip of the Norfolk Ridge reached the trench, the Loyalty Basin lithosphere was obducted without an on land sedimentary record.

The pre-obduction period thus covers the interval between *ca* >56 Ma (subduction inception) and *ca* 34 Ma (final obduction in the south of the island). Tectonic events during this period have been recorded in the Eocene HP-LT metamorphic belt (lower plate) and in the allochthonous Poya Terrane (initially lower plate, then transferred to the upper plate) and Peridotite Nappe (upper plate) of the subduction-obduction system.

Tectonic events will be addressed hereafter in the chronological order (from subduction inception to obduction) and from top to bottom of the tectonic pile (Peridotite Nappe to metamorphic belt).

3. Tectonic records from the Peridotite Nappe

The Peridotite Nappe is formed of a thin (< 2000m) sheet that rests almost horizontally upon underlying terranes (<2° along the west coast), except along the east coast where the basal thrust marked by the serpentinite sole, 20 to 200 m thick, dips 30° on average toward the northeast (Loyalty Basin); (Guillon, 1975). Kinematic indicators from the serpentinite sole generally indicate top-to-the-southwest motion (Gautier et al., 2016; Quesnel et al., 2013; Quesnel et al., 2016); locally however, some evidence for top-to-the-northwest and top-to-the-south motions may correspond to late/local movements of the allochthon.

Internal structure

The geometry of high temperature mantle fabric of the Peridotite Nappe is quite different from that of the basal thrust and the dip of the foliation in peridotite often exceeds 20° forming km-scale open folds and may be upright in the vicinity of large high-temperature shear zones. Until recently, no large internal thrust or detachment fault had been noticed, however, widely spaced shallow dipping discontinuities connected with the sole thrust have been imaged by airborne electromagnetic survey and interpreted as such (Jeppi, 2018). However, such a relatively simple structure sharply contrasts with the imbricate structure of the directly underlying Poya Terrane.

Shear zones

Three regional-scale high-temperature shear zones have been recognized: the Bogota Transform Fault oriented N20°E (Prinzhofer and Nicolas, 1980; Titus et al., 2011), the Bélep Shear Zone oriented N140°E (Nicolas, 1989; Sécherre, 1981; Titus et al., 2011), and the Humboldt Corridor trending N165°E (Ferré et al., 2004; Vogt and Polvin, 1983) (Figure 1). These ductile shear zones are characterized by steeply dipping foliation and horizontal stretching lineation associated with dextral transcurrent motion. The current paleotransform interpretation of these shear zones, which connect laterally with the mantle fabric of Peridotite Nappe, suggests the occurrence of differently oriented spreading ridges, a common feature of back-arc basins (e.g. North Fiji Basin); (Auzende et al., 1995). However, there is no time constraint on the activity of these shear zones and their correlation with either the Late Cretaceous marginal basin stage or the Eocene fore-arc basin stage remains conjectural. Whatever the interpretation, these large-scale discontinuities and the associated fracture network most likely played a role during the pre-obduction period by reorienting local stress and channelizing supra-subduction fluids and magmas (see below). The occurrence of interstitial pargasite/edenite in the sheared peridotite followed by the development of upright lizardite seams parallel to the

foliation recorded fluid-rock interaction at decreasing temperature within the shear zone system (Teyssier et al., 2016).

Dykes

The Peridotite Nappe is intruded by a variety of dykes, which vary in composition from ultramafic (pyroxenite) to mafic (gabbro, diorite, hornblendite, dolerite, boninite), and felsic (leucogabbro, leucodiorite, granite). They all display supra-subduction geochemical features and represent slab melts (adakite series), mantle wedge melts (boninite series) and juvenile mantle melts (island-arc tholeiites) (Cluzel et al., 2006). Their texture is generally coarse to medium-grained except basalt dykes, which display doleritic to microlithic texture. They are found independently of the structural level and nature of the ultramafic host rock (harzburgite, duinite or lherzolite). Dykes never appear in underlying units, notably Poya Terrane, and thus predate subduction as confirmed by geochronological data (Cluzel et al., 2006). In general, the density of dykes, 10 cm to 10 m thick, is greater near the base of Peridotite Nappe except for dolerites which are also present in the upper (cumulate) level of the nappe. The dykes are well preserved in the main body of the ultramafic allochthon and in contrast, severely disrupted in the terrentinite sole.

Due to the large spacing, crosscutting relationships are rarely observed; however, dyke textures allow establishing a rough chronology. Anthophyllite grains of some pyroxenite dykes are nucleated in the harzburgite wall rock, some dykes are boudinaged in a ductile fashion (e.g. Poum Massif, Bogota Peninsula); (Titus et al., 2017) and thus were intruded within a still hot peridotite. In contrast, although coarse-grained, most felsic dykes were emplaced in a colder rock and developed anthophyllite-chlorite reaction rims or no rims. Finally, dolerite/basalt dykes are fine to very fine grained, some display chilled margins and have intruded cold host rocks.

Datable (zircon-bearing) dykes were emplaced between 55.5 Ma and 50 Ma (U-Pb on zircon) and IAT dolerite/basalt dykes at ca 50-47 Ma ($^{40}\text{Ar}/^{39}\text{Ar}$) (Cluzel et al., 2006, 2020 and unpubl. data) within an already existing fracture network of the host rock, as shown by straight boundaries and abrupt direction changes in a clearly dilatational setting (Figure 2).

Fig. 2 Tiebaghi unsheared dykes

Widespread coarse-grained felsic dykes suggest relatively slow cooling. In addition, pegmatitic (Figure 3) and sub-solvus textures and locally retrograde mineral associations suggest involvement of hydrous fluid. Depending on their age and orientation, some dykes underwent internal ductile deformation, which does not exist in the peridotite host (mineral boudinage, mineral preferred orientation, flow folding or microfolding, mylonitisation); (Figure 4 and Figure 5) and a compositional

layering parallel to dyke walls is locally developed, thus suggesting high-temperature shearing and thus magma injection in active faults. Two-step intrusion is recorded by some dykes, which display a foliated part (earlier) while the rest of the dyke (later) displays granular texture (Figure 5). Thus shearing deformation only occurred during the early stage of dyke emplacement, a feature confirmed by radio-chronological data (see below). In contrast, younger IAT dolerite/basalt dykes display chilled margins, finer grain size, and lack secondary minerals. Dolerites have crystallized rapidly and were emplaced at lower temperature (i.e. later than most other dyke types) and in the absence of excess water.

Figures 3, 4 and 5 unsheared and sheared dykes

Dyke orientations do not fit a simple tension crack model since two or more sets of upright dykes commonly coexist (Figure 6). At island scale, there is no clear preferential orientation; however, the dykes roughly cluster at *ca* N130E, N20°E, and N70°E; i.e., parallel or perpendicular to the main lineaments of the Peridotite Nappe. Magma was injected through joints probably formed during the cooling of the ductile shear zones. For example, mafic dykes of the Bogota Peninsula, in spite of some dispersion, cluster at *ca.* N20°E (Titus et al., 2011); (Figure 6), i.e., more or less parallel to the Bogota Shear Zone.

Fig. 6 structural analysis of Eocene dykes

Sheared dykes mainly occur near the base of Peridotite Nappe in the south of the island (Plum Pass, Ouen Island, Casy Islet) but they also occur, although more scarcely, in northern massifs. Dextral motion is recorded by WNW-ESE trending sheared dykes while rare NNW-SSE trending dykes display sinistral motion (Figure 6), thus recording NW-SE directed shortening and NE-SW stretching directions.

Sheared diorite dykes, which occur to the southeast of Noumea (Plum Beach, Massif du Sud) have been dated at *ca* 55 Ma ($^{40}\text{Ar}/^{39}\text{Ar}$ on hornblende); (Soret et al., 2016), which is a minimum age for magma injection and more probably represents the age of shearing deformation. Some amphiboles of the same group of outcrops yielded older Ar/Ar apparent ages (up to 92 Ma) (Soret et al., 2016); however, similar coarse-grained diorite dikes with the same orientation and composition, which crop out along the provincial road to Goro (Plum Pass) a few 100ms from this outcrop, have been dated at *ca* 54 Ma (U-Pb on zircon); (Cluzel et al., 2006). Therefore, anomalously older ages probably recorded some excess radiogenic argon. In fact, the inverse isochron plot (Soret et al., 2016; Figure S1) gives an apparent age of 86.5 ± 7.5 Ma and an intercept corresponding to the atmospheric argon. Ductile deformation of hornblende does not occur below 650–750°C in the presence of an

aqueous fluid (Berger and Stünitz, 1996); therefore, older (Late Cretaceous) ages are likely due to synkinematic high-temperature fluid ingress, undetectable by the step-heating degassing method.

The coexistence of un-sheared nearly orthogonal dykes and specifically in the Massif du Sud, shallow dipping sills on the same sites, is consistent with dilatational conditions (i.e. multi-directional extension) after an early episode of NW-SE directed compression; however, the role of magma overpressure should not be neglected and the abundance of sills may be consistent with compressional context (i.e. vertical minimum stress) as well (Menand et al., 2010).

With the exception of Kopeto Massif where a lenticular NE-dipping dolerite dyke has been injected in a large serpentinitised northeast-dipping normal fault (Figure 7), dolerite dykes remain unaffected by internal deformation. Thus, dyke emplacement in the upper plate started with NW-SE compression and finished with SW-NE extension in a context of decreasing temperature from 55.5 Ma to 50-47 Ma.

Fig. 7 lenticular dolerite dyke (Kopeto Massif)

Antigorite and antigorite-tremolite crack seals

Small faults (shear joints) and tension cracks are widespread in the Peridotite Nappe (Figure 8). They occur by reactivation of lizardite-chrysotile bearing joints and are coated by synkinematic antigorite and antigorite-tremolite-bearing crack seals. Because antigorite and tremolite form at higher temperature than lizardite and chrysotile, the former record syntectonic high-temperature and Ca-rich fluid input. A connection with fluids emitted by the subduction zone, or having leached lower Eocene supra-subduction dykes is suggested by their strontium and oxygen isotope signatures (Cluzel et al., 2019) and this places them within or by the end of the 55-50 Ma interval.

Figure 8 antigorite and tremolite crack seals

Antigorite- and antigorite-tremolite-bearing crack seals do not fit Anderson's model (1951) of synchronous brittle failure and shear motion; instead, they correspond to the reactivation of (lizardite-coated) pre-existing fractures. Their spacing is variable and they may locally appear in swarms as an effect of strain localization due to the proximity of pre-existing regional-scale shear zones (e.g. Bogota Shear Zone, Humboldt Corridor) (Figure 1). The dominant directions of tension cracks/fault are roughly similar to that of supra-subduction dykes as they used the same pre-existing joint network.

The kinematic fault analysis based on fiber axis as a slip vector, shows a predominance of strike-slip and oblique-slip motion, which contrast with the dominant dip-slip motion of supergene faults

(Iseppi et al., 2018). The main axes of the strain ellipsoid (X stretching, Y intermediate, Z shortening) computed with the with FaultKin program (Marrett and Allmendinger, 1990; Allmendinger et al., 2012) show three domains characterized by the orientation of the stretching axis (X) of the strain ellipsoid: Massif du Sud (NNW-SSE), Kopeto-Boulinda and Poro (NNE-SSW), and Koniambo and Tiebaghi (ENW-ESE); (Figure 9). However, it appears that such differences are mainly due to the permutation of the principal strain axes. For example, in the Massif du Sud, the sites of Col Paillard and Vulcain Mine display similar orientation of the main stretching axis (X) while the shortening (Z) and intermediate (Y) axes are permuted. Similarly, Gemini Mine (Kouaoua) and Dunités 78 sites display permuted Y and Z axes (Figure 9). In the north, Koniambo and Tiebaghi sites correspond to the permutation of X (main stretching axis) into Y (intermediate), X and Y being horizontal and X oriented WNW-ESE, i.e. at right angle to its orientation in the Massif du Sud. In the absence of folding or tilting strong enough and oriented accordingly to account for permutation of main strain axes, such apparent complexity may simply result from permutation of principal stress axes (σ_1/σ_2 or σ_2/σ_3) and thus of the principal axes of the resulting strain ellipsoid (X/Y and Y/Z). Such an event may occur in brittle tectonic regime, even during a single-stage tectonic event (Angelier, 1989). The permutation of the main axes of the stress ellipsoid may easily occur at relatively shallow depth when the stress anisotropy is low.

Fig. 9 kinematic analysis of tremolite-antigorite crack seals

The kinematic analysis of antigorite (in) antigorite-tremolite crack seals infers that the Peridotite Nappe (i.e., the upper plate) was in a dominantly extensional or transtensional regime soon after the intrusion of felsic dykes, i.e. less than 6 My after subduction inception.

4. Tectonic records from the Poya Terrane

The allochthonous Poya Terrane (or Poya Nappe) (Cluzel et al., 1997, 2001, 2017) consists of an elongate unit 20 x 180 km located on the west coast and smaller slices along the east coast and Massif du Sud, systematically located beneath the Peridotite Nappe (Figure 1). It is a composite litho-tectonic unit composed of: 1) the Poya Terrane Basalts (PTB), MOR-type massive and pillow basalts associated with Campanian to lower Eocene abyssal argillite (Aitchison et al., 1995; Cluzel et al., 2001; Eissen et al., 1998), and 2) the Kone Facies (KF; Carroué, 1972), upper Cretaceous distal turbidites with minor fine-grained sandstone at the base and dark red or dark grey argillite on top, originally accumulated on the eastern passive margin of the Norfolk Ridge, intruded by 10m to 100m thick lower Eocene E-MORB sills (ca 55 Ma); (Cluzel et al., 2017).

The basal thrust of the main unit forms a gentle synform except in the southern end near Bourail where it tightens above the back limb of the Montagnes Blanches ramp anticline. The top of the unit is formed by the almost horizontal ($<2^\circ$ dip) basal thrust of the Peridotite Nappe. The complex internal structure of PTB, which consists of a stack of upright fault-bounded slices a few meters thick and a few 100 meters long (Figure 10), sharply contrast with the simple geometry of the limiting thrusts. It is worth noting that KF and PTB are not mixed and that the structure of the Kone Facies sub-unit is much simpler than that of PTB, as it lacks multiple tectonic slicing, denoting a distinct and much simpler tectonic evolution. Thus, imbrication of PTB predated amalgamation with KF. The PTB were scraped off the uppermost oceanic crust of the lower plate during the shallow-dipping subduction of the South Loyalty Basin and do not contain any other lithology than basalt and pelagic argillite. The tectonic slices were first accreted to the intra-oceanic fore-arc region of the Loyalty Arc and then thrust over the leading edge of the New Caledonia Ridge (Cluzel et al., 2001). When it reached the margin, the PTB dragged large parts of the passive margin turbidites of the Koné Facies and the whole set was thrust upon autochthonous/parautochthonous rocks of the New Caledonia Ridge where it fed syntectonic foreland basins (Maurizot and Cluzel, 2014). The main unit of the Poya Terrane (west coast) only displays low grade metamorphism (zeolite-chlorite sub-greenschist facies) and thus was not buried deeply, while schistosity is restricted to a narrow zone 200-300m thick beneath the Peridotite Nappe. In contrast, portions of the Poya Terrane (PTB and KF) were dragged down into the subduction zone and recrystallized into blueschists; as a consequence, discontinuous slivers of metamorphosed Poya Terrane rocks crop out along the east coast of New Caledonia (Hienghène region) (Cluzel et al, 2017). Radiochronologic dating of these relatively low grade metamorphic rocks was proven difficult and no reliable data is available that could constrain diachronic accretion.

Fig. 10 typical exposure of Poya Terrane Basalts with upright sedimentary lenses

At island's scale, the orientation of sedimentary lenses in PTB, and of bedding and dolerite sills in KF display an average northwest-southeast strike; however, at all scales, open folds with vertical axes affect the average strike (Figure 11). With only a few exceptions these folds, especially the larger ones (several km), have a "Z" shape consistent with dextral transcurrent tectonics (transpression). However, to the northwest of the unit near Kaala-Gomen the vergence of the large fold is unclear due to the lack of outcrops in the littoral plain (Figure 11). The folds with vertical axes affect the PTB and KF but do not extend into the "autochthonous" basement of the unit, which

displays a relatively simple structure (Figure 11). Thus, transcurrent folding occurred before the final tectonic emplacement of the terrane.

Fig. 11 Tectonic map of the Poya Terrane

The tectonic evolution of the Poya Terrane may therefore be summarized in four steps: 1) shallow-dipping subduction inception (Figure 12a); 2) Intra-oceanic tectonic accretion of the PTB in the fore-arc region (Figure 12b); 3) amalgamation of PTB and KF when the PTB reached the leading edge of the Norfolk Ridge and transcurrent dextral deformation (Figure 12c); and 4) thrusting of the already folded Poya Terrane (PTB + KF) “en bloc” onto the Norfolk Ridge. Meanwhile, elements of the PTB were dragged into the subduction zone with elements of the upper plate (supra-subduction mantle, fore-arc basin) where they recrystallized into blueschists and eclogites as part of the Pouebo Melange (see below) (Cluzel, 2020).

Fig. 12 model for oblique subduction/accretion

5. Tectonic records from the Eocene high pressure – low temperature metamorphic belt

The Eocene metamorphic belt extends over ca 225 km along the northeastern coast of New Caledonia (Fig. 1). Four main lithotectonic units may be distinguished on the basis of lithology and metamorphic grade: (1) Montagnes Blanches Nappe, (2) Diahot-Mt Panié Terrane, (3) Intermediate Melange units, and 4) Pouebo Melange (or Terrane). The metamorphic grade increases along a SW-NE section from sub-greenschist facies (Potel et al., 2006) to eclogite facies (Clarke et al., 1997; Fitzhebert et al., 2003; Vitale Brovarone and Agard, 2013) over a distance of about 20 km. Such a steep increase implies that “isograds” across strike are actually fault/thrust boundaries between sliced units of different yet northeast-ward increasing metamorphic grade (Cluzel et al., 1995; Vitale Brovarone and Agard, 2013). Abrupt changes in style and intensity of ductile deformation are generally associated with these boundaries, which may be or not, associated with serpentinite or mélangé slices. In contrast, the metamorphic grade gently decreases southeastward (along strike); a fact that suggests that subduction was dipping to the north or the north-northeast.

The timing of HP-LT metamorphism is well constrained in high grade units only. The peak metamorphic grade (eclogite facies) in the Pouebo Terrane has been dated at ca 44 Ma (U-Pb zircon) (Spandler et al., 2005), it will be taken as the maximum age for exhumation inception. Eclogite facies rocks of the Diahot-Mt Panié Terrane yielded a younger peak metamorphic age at ca 38 Ma (U-Pb zircon) (Cluzel et al., 2010; Pirard & Spandler, 2017). Both terranes yielded dispersed retrograde

(blueschist/greenschist facies) $^{40}\text{Ar}/^{39}\text{Ar}$ ages on phengite and fuschite that cluster at *ca* 38 Ma (40-28 Ma) (Baldwin et al., 2007; Ghent et al., 1994; Rawling, 1998). Finally, apatite fission tracks yielded an age of 34 ± 4 Ma for a closure temperature of *ca* 150 °C (Baldwin et al., 2007).

The regional foliation associated with tight or isoclinal F1 folds is generally upright, except in the low grades zones. To the southwest across strike, near the peridotite klippe of the west coast, the dip quickly changes into 45° to the northeast. Similarly, the foliation becomes shallow-dipping to the southeast of Touho fault and passes beneath the basal contact of Peridotite Nappe near Ponerihouen (Figures 1 and 13a). The structure of the high grade zone of the Mt Colnet-Mt Panié Massif escapes this general scheme and foliation in the northeastern part of the Diahot-Mt Panié Terrane forms a broad antiform, cored by the Pouebo Melange. The fold type changes with lithology and with metamorphic grade from southwest to northeast, evolving from gentle to isoclinal. Northeastward, i.e. near the higher grade zone, F1 isoclinal folds are refolded in a continuum by tight F2 with roughly the same kinematics, thus resulting in complex outcrop patterns. With only a few local variations due to subsequent F3 folding, the stretching lineation associated with the regional foliation has an average west northwest-east southeast strike (N70°E on average); (Figure 13b), not exactly perpendicular to the orientation of regional structures. The regional foliation strikes northwest-southeast on average; however, at all scales (meter to several kilometers) the F1 and F1-2 fold axial surfaces, and the associated foliation and serpentinite/melange slices display strike changes due to F3 open/close post-foliation folds with vertical axes.

Fig. 13 tectonic map of the Eocene metamorphic belt

At regional scale, three major F3 folds appear in Arama, Ouegoa and Touho-Poindimié areas (Figure 13a). The fold style evolves with metamorphic grade from northwest to southeast (along strike) from close in Arama and Ouegoa areas to the Touho-Poindimié fold-fault (Figure 13a). Similarly, the intensity of deformation associated with these folds decreases southwestwards together with metamorphic grade. Asymmetrical folds with a “Z” shape on map and on outcrop are consistent with dextral transpression (Figure 13b). Regarding the timing, F3 folds involve units of different metamorphic grade, which were previously juxtaposed along faults/thrusts and thus transcurrent folding is late- to post-exhumation (44-34 Ma).

6. Paleomagnetic data

Paleomagnetic studies attempted in New Caledonia (Tarling, 1967; Ali and Aitchison, 2000, 2002; Dallanave et al., 2018, 2020; Théveniaut et al., 2017) have proven difficult due to tectonic

complexity, frequent remagnetization and prominent tropical weathering. With only rare exceptions, pre-Eocene terranes could not provide reliable data, probably due to the thermal effect of the Late Cretaceous rifting. In contrast, Eocene sedimentary rocks yielded some results in spite of feeble remanent magnetization.

The study of Ali and Aitchison (2000, 2002) focused on the early Permian Koh Ophiolite and Poya Terrane Basalts. Permian rocks did not allow a reliable paleomagnetic pole to be computed; however, in spite of tectonic complexity (see below), they could place the origin of Poya Terrane Basalts at about 300 km to the north of present-day New Caledonia.

Dallanave et al. (2018, 2020) carried out a magnetostratigraphic study in mid-Eocene hematite-bearing calciturbidites from Noumea Peninsula and the moderately folded area to the east of Koumac (west coast, north of the island). The former site being an olistolith, the data could not be used for paleomagnetic pole computing; but with the latter (ca. 45 Ma; site X, Fig. 1), a counterclockwise rotation of $\sim 60^\circ$ of New Caledonia with respect to Australia was evidenced and will be used in this article.

In order to test our tectonic interpretation and quantify the rotation at island's scale, a paleomagnetic study has been carried out in the southern half of the island in areas of the west coast that escaped Z-type transcurrent folding and the effects of Eocene HP-LT metamorphism (Fig. 1). All samples were taken in shallow dipping beds on outcrops as fresh as possible with a portable gasoline driller (supplementary material, Table S1). Sampling for this study was performed on upper Eocene turbidites (38-34 Ma) from the Flysch de Bourail near Noumea at Baie de Gadji (site A), along the main road from Bourail to Moindou at Col des Arabes (site E), and Priabonian (ca. 35 Ma) Flysch de Bourail at La Roche Percée (Bourail; site F), Lutetian (42 Ma ?) calcareous sandstones at the base of the Flysch de Bourail at Co. Aymes (site G) and lower Eocene dolerite (ca. 50 Ma) from the Peridotite Nappe (Tontouta River, site H). Rocks from the sites G and H provided dispersed directions that could not be used in this study. Owing to the uncertainty of stratigraphic correlation of turbidites, an average age of 35 Ma was collectively attributed to the three sites. Triassic to Paleocene formations were also sampled for paleomagnetic analysis but yielded complex remagnetization features, the analysis of which does not meet the aims of this article.

Details on the laboratory paleomagnetic analyses are provided as online supplementary information.

Magnetite with low concentration has been identified as the major magnetic remanence carrier by the hysteresis curve acquisition, thermo-magnetic experience and isothermal magnetic

remanence measurement (Fig. S1). The degree of Anisotropy of Magnetic Susceptibility is less than 1.05 (Fig. S2), indicating that the sampled rocks have not experienced severe deformation after diagenesis. The remanence measurement of progressive demagnetization confirms weak magnetization ($\sim 10^{-4}$ Am² for NRM; Fig. S3). Less than 50% of demagnetized specimens from only three sites present stable Characteristic Remanence Magnetization (ChRM), and two other sites did not provide any stable magnetic remanence (Table 1).

Table 1. Paleomagnetic results from southern New Caledonia. n/N, D, I, α , g and s stand for statistic/total measured samples, declination, inclination cone radius of statistic confidence at 95%, in-situ, bedding-corrected coordinates, respectively.

It is worth to note that: i) the directions of these sites are relatively compatible; ii) due to the small number of available specimens taken in statistical analysis from each site, the statistical confidence level is relatively low; iii) due the small number of sites, the age averages are calculated by specimen instead of site. Nevertheless, the age average provides reasonable results with acceptable statistical confidence level (Table 1). Because of the good compatibility among the three sites, one general average has been calculated for the age of ~ 35 Ma: $D_g = 341.1^\circ$, $I_g = -31.8^\circ$, $k = 9.0$, $\alpha_{95g} = 14.0^\circ$; $D_s = 345.9^\circ$, $I_s = -36.7^\circ$, $k = 11.0$, $\alpha_{95s} = 12.5^\circ$ and $n = 14$ (Table 1 and Fig. 14).

Figure 14. Equal-area projection of directions from Characteristic Remanence Magnetization (ChRM). a. directions in in-situ coordinates; b. directions in bedding corrected coordinates.

The fold test (McElinny, 1964; McFadden and McElinny, 1990) provides an inclusive answer due to weak variation of bedding attitude; nevertheless, an improved precision parameter is obtained after bedding correction (Table S1 and Fig. S4). With both normal and reversed magnetic polarities, the ChRM could be considered as primary magnetization (Figs. S3 and S4). Accordingly, a paleomagnetic pole has been calculated at: $\lambda = 78.6^\circ$, $\phi = 80.4^\circ$, $dp = 6.8^\circ$; $dm = 11.6^\circ$ (Table 2).

Table 2. Comparison of paleomagnetic results from New Caledonia with Australian APWP

This new pole is not only distinct from that of the present Earth field, but also from that of Australia at ~ 35 Ma (Fig. 15); (Besse & Courtillot, 2002, 2003). It also differs from the paleopole

computed from slightly older sediments (ca. 45 Ma) near Koumac in the north of New Caledonia (Dallanave et al., 2020; see (Fig. 1, site X) and Fig.15). Table 2 reports their angular differences and their latitude and rotation components showing that latitudinal movements between New Caledonia and Australia are not really significant compared to rotations. Assuming the primary origin of ChRM of paleomagnetic data from New Caledonia, the new results show an counterclockwise rotation of $-31.2^{\circ} \pm 9.6^{\circ}$ since 35 Ma of New Caledonia with respect to Australia, confirming the tectonic evolution suggested by observations from other domains (Fig. 16).

However, there is a statistically significant difference between the southern part (this study) and the northern part of the island (Dallanave et al., 2020) with a bulk angular difference of $32.5^{\circ} \pm 8.3^{\circ}$ between their paleomagnetic poles (Table 2). Such a difference may be produced by: 1) local rotations due to transcurrent folding (folds with vertical axes), 2) differential rotation between the north and the south of the island; or, 3) progressive rotation through time. As described above (paragraph 5), the studied terranes have experienced superposed deformations and especially folding with vertical axes that may account for local rotations (Fig. 13). The results from the northern site (site X; Dallanave et al., 2020) are derived from a magnetostratigraphic study, and thus correspond to a restricted area of a few hundred square meters, lacking visible metamorphism and ductile deformation. The studied sequence is moderately dipping ($\sim 30^{\circ}$ to the NE) and monoclinical, preventing any fold test to be performed. However, the strike of F1-2 fold axes remains constant in this area over more than 20 km and there is no evidence for F3 transcurrent folds with vertical axes (see paragraph 5). Results of this study come from large monoclines, several km across strike, which show no evidence for transcurrent folds and thus no local rotation around vertical axes. The paleomagnetic data from the studied areas may suggest that counterclockwise rotation of the northern part of the island was larger than that of the southern part; however, the island does not show bending at that scale, which could account for $\sim 30^{\circ}$ differential rotation. An alternative interpretation may be proposed in term of chronology. The paleomagnetic data of Dallanave et al. (2020) are dated at ~ 45 Ma by micropaleontology and magnetostratigraphy, and show a counterclockwise rotation of $\sim 60^{\circ}$ of New Caledonia with respect to Australia, which is about 30° more compared to our results from rocks dated at ca. 35 Ma (Table 3). In other words, New Caledonia began its counterclockwise rotation with respect to Australia after ca. 45 Ma ($\sim 30^{\circ}$) and continued after 35 Ma ($\sim 30^{\circ}$). Since no rotation relative to Australia was observed in the paleomagnetic record of Oligocene lateritic cuirasses (>25 Ma; Sevin et al., 2012) or late Oligocene granitoids (~ 25 Ma; Théveniaud et al., 2017), counterclockwise rotation ceased before 25 Ma. Unfortunately there is no on land sedimentary record for the period of 35-25 Ma and thus no precise constraint on the end of rotation. Owing to the small number of data, it clearly appears that these

results are only qualitative and need to be comforted by a larger number of samples. However, evidence for about 60° counterclockwise rotation, also reported by Théveniaut et al. (2017) supports the tectonic model presented below.

7. Discussion: chronology and kinematics

From subduction inception to obduction and from top to bottom of the tectonic pile, significant changes were recorded through time by pre-obduction tectonic events (Table 3). The oldest events associated with subduction inception did not leave any trace useful for kinematic analysis because they were greatly disturbed and possibly rotated by subsequent events (metamorphic sole) or disrupted by the melange process (earliest supra-subduction dykes and fore-arc basin rocks). Pyroxenite dykes and small-scale intrusions could not be dated and thus are difficult to relate to a given tectonic event. The earliest datable tectonic events appeared in the Peridotite Nappe with lower Eocene sheared dykes (55.5-55 Ma), which unexpectedly recorded NW-SE-directed compression and strike-slip motion. This event was short-lived and in the rest of the dyke complex emplacement period (55-50 Ma), wrench tectonics changed into multidirectional extension (dilatation). However, the role of magma pressure in this evolution should not be neglected because it tends to reduce the stress anisotropy and may have resulted in nearly isotropic dilatation while the external stresses at regional scale remained unchanged. From 55 Ma to 50 Ma, however, the grain size reduction and appearance of non-reactional chilled margins signal relatively fast cooling of the fore-arc. In addition to a change in the magma source, island-arc dolerites, which emplaced from 50 Ma to 47 Ma, recorded WNW-ESE directed extension (Bogota Peninsula) or SW-NE directed extension (Kopeto Massif).

Antigorite- and tremolite-bearing crack seals recorded either transtension or nearly N-S extension depending upon the place, as a consequence of principal stress permutation. The poorly fixed orientation of kinematic axes suggests low anisotropy of the stress ellipsoid and thus relatively shallow depth due to peridotite exhumation. Pre-existing discontinuities (e.g. regional-scale shear zones) may be suspected to have re-oriented the local stresses. In spite of some uncertainty on boundaries, the mineral sequence, i.e. lizardite (\pm chrysotile) => antigorite+ tremolite => antigorite => polygonal serpentine, provides some constraints on the evolution in temperature. The upper stability limit of lizardite (\pm chrysotile) at low pressure (< 0.4 GPa) is established to about 300-320°C (Evans, 2004), while antigorite stability starts at about 320°C and persists up to 500-550°C (Wenner and Taylor, 1971). At low to medium pressure (0.1-0.5 GPa) tremolite appears at 350-550°C and disappears at 400-650°C depending on the CO₂ partial pressure (Jenkins, 1983; Chernosky et al., 1998; Evans, 2004; Evans et al., 2000, 2013). Therefore, the relative chronology above records: 1) a net increase in temperature after primary serpentinization due to the ingress of slab-derived fluids

during the formation of tremolite-antigorite bearing veins, 2) a gentle temperature decrease at the end of tremolite crystallization, and 3) a final cooling down to supergene conditions (ca. 50°C-35°C) (Cluzel et al., 2019). The predominance of strike-slip or oblique slip displacements denotes transtensional conditions in the upper plate consistent with oblique subduction (Chemenda et al., 2000; Gurnis et al., 2004; Gutscher et al., 1998, 2000).

In contrast with the weak and poorly time-constrained tectonics of the upper plate, the HP-LT belt and Poya Terrane display spectacular tectonic features, which directly relate to a specific tectonic event. Stacking and exhumation of HP-LT units probably occurred with a dominant ENE-WSW (N70°E) direction recorded by the regional stretching lineation (Figure 13c, Table 3).

Notwithstanding the subsequent deformation by folds with vertical axes, the initial orientation of the tectonic slices of the Poya Terrane was similar to that of the metamorphic belt (i.e. NW-SE in the present configuration of the island). Both terranes display the same “Z”-type folds denoting dextral transcurrent tectonics by the end of exhumation in the HP-LT belt and before final overthrusting of the Poya Terrane (Figure 13 & Table 3).

Table 3 summary of Eocene tectonic events

Since transcurrent deformation is not expected to occur during SW-directed (i.e. at right angle) overthrusting, it is assumed that dextral shearing occurred before the island’s scale counterclockwise rotation while the Australian Plate was moving northwards with respect to the coeval Loyalty Volcanic Arc. Counterclockwise rotation of the northern Norfolk Ridge and coeval clockwise rotation of the D’Entrecasteaux zone were responsible to the hook shape of the Loyalty-D’Entrecasteaux subduction zone. Therefore, it is likely that the northern Norfolk Ridge originally had an almost north-south direction, more consistent with the reconstruction of the ancient Gondwana margin than the present-day NW-SE orientation (Figure 16a). The unexpected shortening direction (NW-SE) recorded by sheared dykes emplaced shortly after subduction inception was possibly due to north-directed subduction if the island is rotated back to its original N-S orientation. Oroclinal bending of the ridge could not be achieved without crust-mantle detachment (not to say subduction) along its western edge, and was made possible by the narrowness (< 100 km) of the continental Norfolk Ridge; this point is supported by paleomagnetic data, which records post-mid-Eocene counterclockwise rotation of about 60° (Dallanave et al., 2020; this study). Obduction of the Peridotite Nappe occurred during this rotation (Figure 16c).

Obduction was achieved after ca 34 Ma in the south of the island (Cluzel et al., 1998) and continued farther south (Patriat et al., 2018) for an unknown period of time. Finally, to the southwest of New Caledonia, the incipient collision (or failed continental subduction) of the Lord Howe Rise

with the northern Norfolk Ridge (Figure 16d) recorded by the local north-eastward dip of the Moho and uplift of Fairway Ridge, likely resulted in final blocking of the subduction at the latitude of New Caledonia. As a consequence, increasingly fast eastward rollback of the VTK subduction in Oligocene time (> 30 Ma; van de Langemaat et al., 2018) accompanied the continuous opening of the North Loyalty/South Fiji back-arc basin.

8. *Fig. 16 model for the evolution of the SW Pacific between 56 Ma and 30 Ma*

Conclusions

From subduction inception to obduction, tectonics occurred at decreasing temperature and pressure in the Peridotite Nappe (upper plate) and in the HP-LT metamorphic belt (lower plate part). Such decrease associated with exhumation of the HP-LT belt and uplift of Peridotite Nappe is recorded by the changing style of tectonic structures and associated mineralization (Table 3).

Shortly after subduction inception, the shortening direction recorded by deformed lower Eocene dykes in the upper plate was parallel to the present NW-SE strike of the island. Owing to the counterclockwise rotation deciphered by paleomagnetic data during the 45-25 Ma time interval, the shortening direction was roughly oriented N-S at start and the Australian Plate was moving northwards with respect to the Pacific Plate.

Distal turbidites of the late Cretaceous passive margin (Kone Facies) were intruded by prominent lower Eocene (*ca.* 55 Ma) E-MORB dolerite sills. This feature is consistent with extension (bulging and/or transtension ?) in the lower plate (Australian Plate) of the system (Cluzel et al., 2017) shortly after subduction inception.

The progressive counterclockwise oroclinal bending of the New Caledonia/northern Norfolk Ridge due to the blocking of this narrow slice of continental crust in the subduction zone could not be achieved without SE-propagating jump-back of the subduction. Thus, the northern Norfolk Ridge was sandwiched between two lithospheres: the Loyalty fore-arc to the NE and the Australian Plate to the SW, which moved obliquely to each other. Counterclockwise rotation of the New Caledonia Ridge was achieved through rotation around a vertical axis located on the ridge at about 23°S latitude. This point actually correspond to the southern end of the negative gravity anomaly, which follows the ridge for about 800 km to about 18°S and less continuously along the hook-shaped D'Entrecasteaux Ridge where it disappears beneath the Vanuatu trench at about 15°S.

Slices of Poya Terrane Basalts, which were scrapped off from the crust of the lower plate (South Loyalty Basin) and accreted to the Loyalty fore-arc were amalgamated with Late Cretaceous turbidites of the ancient passive margin (Kone Facies) and affected by dextral Z-type transcurrent folds before being thrust "en bloc" in mid-Eocene times, thus recording a change in kinematics due to slab roll back, progressive opening of the North Loyalty back-arc basin and coeval rotation of the Loyalty Arc.

By the end of exhumation of the HP-LT terranes, which started after 44 Ma (Spandler et al., 2005) and was almost completed at *ca.* 34 Ma (Baldwin et al., 2007), the development of dextral

transcurrent folding in the metamorphic belt signals that transpression and thus oblique subduction was continuing.

Younger strike-slip faults that crosscut the Peridotite Nappe front and post-obduction granitoids suggest ongoing post-obduction transcurrent tectonics (transtension ?), which is however beyond the scope of this article.

Acknowledgements

Parts of this study come from M.I. PhD thesis co-funded by BRGM, UNC, the Geological Survey of New Caledonia and CNRT "Nickel et son Environnement" (project Cyprien Struct). M.I. warmly thanks B. Lebayon, and D. Lahondère (BRGM), S. Lesimple, P. Maurizot and E. Robineau (SGNC) for welcome during her stay in New Caledonia, communicating some structural data and assistance in the field. The nickel mining companies of New Caledonia are also collectively acknowledged for permitting access and logistical support during field work in mine sites. LABEX VOLTAIRE (ANR-10-LABX-100-01) and EQUIPEX PLANET (ANR-11-EQPX-0036) are appreciated. Comments by anonymous reviewer are also greatly appreciated.

Credit Author Statement

D. Cluzel : conceptualization, field investigation, paleomag sampling, map analysis, writing and designing ; M. Iseppi : field investigation, kinematic fault analysis ; Y. Chen : paleomagnetic analysis, writing supplementary data section

Declaration of interests

The authors declare that they have no known competing financial interests or personal relationships that could have appeared to influence the work reported in this paper.

References

Aitchison, J., Clarke, G., Meffre, S. and Cluzel, D. (1995). Eocene arc-continent collision in New Caledonia and implications for regional southwest Pacific tectonic evolution. *Geology*, 23, 161-164. [https://doi.org/10.1130/0091-7613\(1995\)023<0161:EACCIN>2.3.CO;2](https://doi.org/10.1130/0091-7613(1995)023<0161:EACCIN>2.3.CO;2)

Ali J.R., and Aitchison J.C. (2000). Significance of palaeomagnetic data from the oceanic Poya Terrane, New Caledonia, for SW Pacific tectonic models. *Earth and Planetary Science Letters* 177, 153-161. [https://doi.org/10.1016/S0012-821X\(00\)00042-1](https://doi.org/10.1016/S0012-821X(00)00042-1)

Ali J.R., and Aitchison J.C. (2002). Paleomagnetic tectonic study of the New Caledonia Koh Ophiolite and the mid-Eocene obduction of the Poya Terrane. *New Zealand Journal of Geology and Geophysics* 45, 313-322. <https://doi.org/10.1080/00288306.2002.9514976>

Allmendinger, R. W., Cardozo, N., and Fisher, D. M. (2011). *Structural geology algorithms: Vectors and tensors*. Cambridge University Press. <https://doi.org/10.1017/CBO9780511920202>

Anderson, E.M. (1951). *The Dynamics of Faulting*, 206 pp., Oliver and Boyd, London

Angelier J. (1989). From orientation to magnitudes in paleostress determinations using fault slip data. *Journal of Structural Geology* 11, 1–2, 37-50. [https://doi.org/10.1016/0191-8141\(89\)90034-5](https://doi.org/10.1016/0191-8141(89)90034-5)

Auzende J.-M., Pelletier B., and Eissen J.-P. (1995). The North Fiji Basin : geology, structure and geodynamic evolution. In : Taylor B. (Ed.) *Back-arc Basin : tectonics and magmatism*. Plenum Press, New York, 139-175.

Avias J. (1967). Overthrust structure of the main ultrabasic New Caledonian massives. *Tectonophysics*, 4, 4-6, 531-541. [https://doi.org/10.1016/0040-1951\(67\)90017-0](https://doi.org/10.1016/0040-1951(67)90017-0)

Baldwin, S.L., Rawling, T. & Fitzgerald, P.G. (2007). Thermochronology of the New Caledonian high-pressure terrane: Implications for middle Tertiary plate boundary processes in the southwest Pacific. *Geological Society of America Special Papers*, 419, 117-134.

Berger A. and Stünitz H. (1996). Deformation mechanisms and reaction of hornblende: examples from the Bergell tonalite (Central Alps). *Tectonophysics* 257, 2–4, 149-174
[https://doi.org/10.1016/0040-1951\(95\)00125-5](https://doi.org/10.1016/0040-1951(95)00125-5)

Besse, J., and Courtillot V. (2002). Apparent and true polar wander and the geometry of the geomagnetic field over the last 200 Myr, *J. Geophys. Res.*, 107(B11), 2300,
<https://doi.org/10.1029/2000JB000050>

Besse J. and Courtillot V. (2003). Correction to “Apparent and true polar wander and the geometry of the geomagnetic field over the last 200 Myr”, *J. Geophys. Res.*, 108(B10), 2469,
<https://doi.org/10.1029/2003JB002684>

Bitoun, G., and Récy, J. (1982). Origine et évolution du bassin des Loyauté et de ses bordures après la mise en place de la série ophiolitique de Nouvelle-Calédonie. Contribution à l'étude géodynamique du sud-ouest Pacifique. *Travaux et documents ORSTOM*, Paris, 505–539.

Briggs, R.M., Lillie, A.R. and Brothers, R.N. (1978). Structure and high-pressure metamorphism in the Diahot region northern New Caledonia. *Bulletin of the BGRM*, Section IV, 3, 171-189.

Carroué J. P. (1972). Carte et notice explicative de la carte géologique de la Nouvelle-Calédonie à l'échelle du 1/50000: feuille Pouembout. Bureau de Recherches Géologiques et Minières, Orléans France.

Carson, C.J., Powell R., Clarke C.L. (1999). Calculated mineral equilibria for eclogites in CaO-Na₂O-FeO-MgO-Al₂O₃-SiO₂-H₂O: application to the Pouebo Terrane, Pam Peninsula, New Caledonia. *Journal of Metamorphic Geology*, 17, 9-24. <https://doi.org/10.1046/j.1525-1314.1999.00177.x>

Chemenda A., Lallemand S., Bokun A. (2000). Strain partitioning and interplate friction in oblique subduction zones: Constraints provided by experimental modeling. *Journal of Geophysical Research* 105, B3, 5567-5581. <https://doi.org/10.1029/1999JB900332>

Chernosky J.V., Berman R.G., and Jenkins D.M. (1998). The stability of tremolite: new experimental data and a thermodynamic assessment. *American Mineralogist* 83, 726-739.
<https://doi.org/10.2138/am-1998-7-805>

Clarke G., Aitchison J.C., and Cluzel D. (1997). Eclogites and blueschists of the Pam Peninsula, NE New Caledonia: a reappraisal. *Journal of Petrology* 38, 7, 843-876.
<https://doi.org/10.1093/etroj/38.7.843>

Cluzel D. (2020). Subduction erosion; contributions of footwall and hanging wall to subduction melange; field, geochemical and radiochronological evidence from the Eocene HP-LT belt of New Caledonia. *Australian Journal of Earth Sciences* 68, 1, 99-119.

<https://doi.org/10.1080/08120099.2020.1761876>

Cluzel D., Aitchison J., Clarke G., Meffre S. et Picard C. (1995). Dénudation tectonique du complexe à noyau métamorphique de haute pression tertiaire (Nord de la Nouvelle-Calédonie, Pacifique, France), Données cinématiques. *Comptes Rendus Académie des Sciences Paris* 321, 57-64

Cluzel D., Picard C., Aitchison J., Laporte C., Meffre S. and Parat F. (1997). La Nappe de Poya (ex-Formation des basaltes) de Nouvelle-Calédonie (Pacifique SW), un plateau océanique Campanien-Paléocène supérieur obducté à l'Eocène supérieur. *Comptes Rendus Académie des Sciences Paris*. 324, 443-451.

Cluzel D., Chiron D. et Courme M.D. (1998). Discordance de l'Eocène supérieur et événements pré-obduction en Nouvelle-Calédonie (Pacifique sud-ouest). *Comptes Rendus Académie des Sciences Paris* 327, 485-91.

Cluzel D., Aitchison J.C., and Picard C. (2001). Tectonic accretion and underplating of mafic terranes in the Late Eocene intraoceanic fore-arc of New Caledonia (Southwest Pacific). *Geodynamic implications. Tectonophysics* 340, 1-2, 23-60. [https://doi.org/10.1016/S0040-1951\(01\)00148-2](https://doi.org/10.1016/S0040-1951(01)00148-2)

Cluzel D., Meffre S., Maurizot P., Crawford A.J. (2006). Earliest Eocene (53 Ma) convergence in the Southwest Pacific; evidence from pre-obduction dikes in the ophiolite of New Caledonia. *Terra Nova*, 18, 395-402. <https://doi.org/10.1111/j.1365-3121.2006.00704.x>

Cluzel, D., Adams, C.L., Meffre, S., Campbell, H.J. and Maurizot, P. (2010). Discovery of Early Cretaceous Rocks in New Caledonia: New Geochemical and U-Pb Zircon Age Constraints on the Transition from Subduction to Marginal Breakup in the Southwest Pacific. *Journal of Geology*, 118, 381-397, <https://doi.org/10.1086/652779>

Cluzel D., Maurizot P., Collot J. and Sevin B. (2012a). An outline of the Geology of New Caledonia; from Permian-Mesozoic Southeast-Gondwanaland active margin to Tertiary obduction and supergene evolution. *Episodes* 35, 1, 72-86. <http://doi.org/10.18814/epiiugs/2012/v35i1/007>

Cluzel D., Jourdan F., Meffre S., Maurizot P., and Lesimple S. (2012b). The metamorphic sole of New Caledonia ophiolite; $^{40}\text{Ar}/^{39}\text{Ar}$, U-Pb, and geochemical evidence for subduction inception at a spreading ridge. *Tectonics*. 31, 3, <https://doi.org/10.1029/2011TC003085>, 2012

Cluzel D., Whitten M., Meffre S., Aitchison J.C., and Maurizot P. (2017). A reappraisal of the Poya Terrane (New Caledonia). Accreted Late Cretaceous marginal basin upper crust, passive margin sediments and Eocene E-MORB sill complex. *Tectonics* 37, 1, 48-70.

<https://doi.org/10.1002/2017TC004579>

Cluzel D. and Meffre S. (2018). In search of Gondwana heritage in the Outer Melanesian Arc: no pre-Upper Eocene detrital zircons in Viti Levu river sands (Fiji Islands). *Australian Journal of Earth Sciences* 66(2), 265-277. <https://doi.org/1080/08120099.2019.1531924>

Cluzel D., Boulvais Ph., Iseppi M., Lahondère D., Lesimple S., Maurizot P., Paquette J.L., Tarantola A., and Ulrich M., (2019). Slab-derived origin of tremolite-antigorite veins in a supra-subduction ophiolite; the Peridotite Nappe (New Caledonia) as a case study. *International Journal of Earth Sciences* 109(1), 171-196 <https://doi.org/10.1007/s00531-019-01726-6>

Collot J.Y., Malahoff A., Recy J., Latham G., and Missegue F. (1987). Overthrust emplacement of New Caledonia ophiolite : geophysical evidence, *Tectonics*, 6, 3, p. 215-232.

<https://doi.org/10.1029/TC006i003p00215>

Collot, J., Geli L., Lafoy Y., Vially R., Cluzel D., Klingelhoefer F., and Nouzé H. (2008). Tectonic history of northern New Caledonia Basin from deep offshore seismic reflection: Relation to late Eocene obduction in New Caledonia, southwest Pacific, *Tectonics*, 27, TC6006,

<https://doi.org/10.1029/2008TC002263>

Dallanave, E., Agnini C., Pascher K.M., Maurizot P., Bachtadse V., Hollis C.J., Dickens G.R., Collot J., and Monesi E. (2018). Magneto biostratigraphic constraints of the Eocene micrite-calciturbidite transition in New Caledonia : tectonic implications, *New Zealand Journal of Geology and Geophysics*, 61(2), 145-163, <https://doi.org/10.1080/00288306.2018.1443946>

Dallanave, E., Maurizot, P., Agnini, C., Sutherland, R., Hollis, C. J., Collot, J., et al. (2020). Eocene (46-44 Ma) onset of Australia-Pacific plate motion in the southwest Pacific inferred from stratigraphy in New Caledonia and New Zealand. *Geochemistry, Geophysics, Geosystems*, 21, e2019GC008699.

<https://doi.org/10.1029/2019GC008699>

DIMENC, Gouvernement de la Nouvelle-Calédonie, online geological map of New Caledonia

<https://dtsi-sgt.maps.arcgis.com/apps/webappviewer/index.html> accessed 03/2020-05/2020.

Espurt, N., Funicello, F., Martinod, J., Guillaume, B., Regard, V., Faccenna, C., and Brusset, S., (2008). Flat subduction dynamics and deformation of the South American plate: Insights from analog modeling: *Tectonics*, v. 27, TC3011, <https://doi.org/10.1029/2007TC002175>

Eissen, J.P., Crawford, A.J., Cotten J., Meffre S., Bellon H., and Delaune M. (1998). Geochemistry and tectonic significance of basalts in the Poya Terrane, New Caledonia. *Tectonophysics*, 284, 203-219. [https://doi.org/10.1016/S0040-1951\(97\)00183-2](https://doi.org/10.1016/S0040-1951(97)00183-2)

Evans B.W. (2004). The serpentinite multisystem revisited: chrysotile is metastable, *International Geology Review* 46:6, 479-506. <http://dx.doi.org/10.2747/0020-6814.46.6.479>

Evans B.W., Ghiorso M.S., and Kuehner S.M. (2000). Thermodynamic properties of tremolite: A correction and some comments. *Amer. Miner.* 85, 3-4, 466-472. <https://doi.org/10.2138/am-2000-0407>

Evans B. W., Hattori K., and Baronnet A. (2013). Serpentinite: What, Why, Where? *Elements* 9, 99-106. <https://doi.org/10.2113/gselements.9.2.99>

Ferré, E.C., Belley, F., Tikoff, B., Martín-Hernández, F., Ninkwe, G. and Ward, C. (2004). Anatomy of an oceanic mantle shear zone deduced from high-field magnetic anisotropy: the Humboldt corridor, New Caledonia. *Eos Trans. AGU*, 85(47), Fall Meeting Supplement, Abstract GP23B-04.

Fitzherbert, J.A., Clarke, G.L. and Powell, R. (2003). Lawsonite-Omphacite-bearing metabasites of the Pam Peninsula, NE New Caledonia: Evidence for disrupted blueschist- to eclogite-facies conditions. *Journal of Petrology*, 44, 1807-1831. <https://doi.org/10.1093/petrology/egg060>

Gautier, P., Quesnel, B., Boulvais, F. and Cathelineau, M. (2016). The emplacement of the Peridotite Nappe of New Caledonia and its bearing on the tectonics of obduction. *Tectonics*, <https://doi.org/10.1002/2016TC004218>

Ghent, E., Roddick, J. and Black, P. M. (1994). $^{40}\text{Ar}/^{39}\text{Ar}$ dating of white micas from the epidote to the omphacite zones, northern New Caledonia: tectonic implications. *Canadian Journal of Earth Sciences*, 31, 995-1001.

Guillon, J.H. (1975). Les massifs péridotitiques de Nouvelle-Calédonie; Type d'appareil ultrabasique stratiforme de chaîne récente. *Mémoire ORSTOM, Paris*, 76, 1-72.

Gurnis, M., Hall C., and Lavie L. (2004), Evolving force balance during incipient subduction, *Geochem. Geophys. Geosyst.*, 5, Q07001, <https://doi.org/10.1029/2003GC000681>

Gutscher M.A., Kukowski N., Malavieille J. and Lallemand S. (1998). Material transfer in accretionary wedges from analysis of a systematic series of analog experiments. *Journal of Structural Geology* 20, 4, 407-416. [https://doi.org/10.1016/S0191-8141\(97\)00096-5](https://doi.org/10.1016/S0191-8141(97)00096-5)

Gutscher M.A, Spakman W., Bijwaard H., and E. Engdahl R. (2000). Geodynamics of flat subduction: Seismicity and tomographic constraints from the Andean margin. *Tectonics* 19, 5, 814-833. <https://doi.org/10.1029/1999TC001152>

Iseppi M. (2018). Fracturation polyphasée et contrôles des gisements de nickel supergène de Nouvelle-Calédonie. Nouvelles méthodes d'exploration et modèles de gisements. PhD thesis University of New Caledonia. 301 p.

Iseppi M., Sevin B., Cluzel D., Le Bayon B. and Maurizot P. (2018). Supergene nickel ore deposits controlled by gravity-driven faulting and slope failure (Peridotite Nappe, New Caledonia). *Economic Geology* 113, 2. <https://doi.org/10.5382/econgeo.2018.4561>

Jenkins D.M. (1983). Stability and composition relations of calcic amphiboles in ultramafic rocks *Contributions to Mineralogy and Petrology* 83, 3-4, 375-384, <https://doi.org/10.1007/BF00371206>

Klingelhoefer, F., Lafoy Y., Collot J., Cosquer E., Géli J., Nozizé H., and Vially R. (2007), Crustal structure of the basin and ridge system west of New Caledonia (southwest Pacific) from wide-angle and reflection seismic data, *J. Geophys. Res.*, 112, B11102, <https://doi.org/10.1029/2007JB005093>

Lahondère D. (2012). Atlas des occurrences et des types de fibre d'amiante sur mine. Rapport BRGM/RP-61426-FR, final report.

Lillie A. R. and Brothers R. N. (1970). The geology of New Caledonia, *New Zealand Journal of Geology and Geophysics*, 13:1, 145-183, <https://doi.org/10.1080/00288306.1970.10428210>

Luyendyk, B. P. (1995). Hypothesis for Cretaceous rifting of east Gondwana caused by subducted slab capture. *Geology*, 23(3), 373-376, [https://doi.org/10.1130/G017613\(1995\)023<0373:HFCROE>2.3.CO;2](https://doi.org/10.1130/G017613(1995)023<0373:HFCROE>2.3.CO;2)

Marrett, R.A. and Allmendinger, R.W. (1990). Kinematic analysis of fault-slip data. *Journal of Structural Geology*, 12, 973-986. [http://dx.doi.org/10.1016/0191-8141\(90\)90093-E](http://dx.doi.org/10.1016/0191-8141(90)90093-E)

Maurizot P. (2011). First sedimentary records of the pre-obduction convergence in New Caledonia: Formation of an accretionary complex during early Eocene in the North of the Grande Terre and emplacement of the Montagnes Blanches nappe. *Bulletin de la Société Géologique de France*, 182(6): 479–491. <https://doi.org/10.2113/gssgfbull.182.6.479>

Maurizot P., Eberlé J.M., Habault C., and Tessarolo C. (1989). Carte géologique Territoires d'Outre-Mer, Nouvelle-Calédonie (1/ 50000), feuille Pam-Ouégoa, 2e édition, B.R.G.M. France. Notice explicative par Maurizot P., Eberlé J.M., Habault C., Tessarolo C., 81p.

Maurizot P., and Vendé-Leclerc M. (2009). New Caledonia geological map, scale 1/500 000, DIMENC - SGNC, BRGM. Explanatory note by Maurizot P. and Collot J.

Maurizot, P., and Cluzel, D. (2014). Pre-obduction records of Eocene foreland basins in central New Caledonia (Southwest Pacific); an appraisal from surface geology and Cadart 1 borehole data. *New Zealand Journal of Geology and Geophysics*, 57, 3, 307-311.
<https://doi.org/10.1080/00288306.2014.885065>

Maurizot, P., Cluzel, D., Meffre, S., Campbell, H.J., Collot, J., and Sevin, B. (2020a). Pre-Late Cretaceous basement terranes of the Gondwana active margin of New Caledonia. In: Maurizot P., and Mortimer, N. (ed.) *New Caledonia: Geology, Geodynamic Evolution and Mineral Resources*. Geological Society, London, Memoirs, 51. <https://doi.org/10.1144/M51-2016-11>

Maurizot, P., Bordenave, A., Cluzel, D., Collot, J., and Etienne, S. (2020b). Late Cretaceous to Eocene cover of New Caledonia: from rifting to convergence. In: Maurizot P., and Mortimer, N. (ed.) *New Caledonia: Geology, Geodynamic Evolution and Mineral Resources*. Geological Society, London, Memoirs, 51, <https://doi.org/10.1144/M51-2017-18>

Maurizot, P., Cluzel, D., Patriat, M., Collot, J., Iseppi, M., Lesimple, S., Secchiari, A., Bosch, D., Montanini, A., Macera, P., and Davies, H.L. (2020c). The Eocene Subduction-Obduction Complex of New Caledonia. In: Maurizot P., and Mortimer, N. (ed.) *New Caledonia: Geology, Geodynamic Evolution and Mineral Resources*. Geological Society, London, Memoirs, 51, <https://doi.org/10.1144/M51-2018-70>

McElhinny, M. W. (1964). Statistical significance of the fold test in palaeomagnetism. *Geophysical Journal International*, 8(3), 338-340. <https://doi.org/10.1111/j.1365-246X.1964.tb06300.x>

McFadden P.L. and McElinny M.W. (1990). Classification of the reversal test in paleomagnetism, *Geophys. J. Int.*, 103, 725-729. <https://doi.org/10.1111/j.1365-246X.1990.tb05683.x>

Meffre, S. (1995). The development of island-arc related ophiolites and sedimentary sequences in New Caledonia. PhD thesis, University of Sydney, Australia, 258 pp.

Meffre S., Crawford A.J., and Quilty P.J. (2006). Arc-continent collision forming a large island between New Caledonia and New Zealand in the Oligocene. ASEG 18th Geophysical Conference Melbourne 2006. ASEG Extended Abstracts <https://doi.org/10.1071/ASEG2006ab111>

Menand T., Daniels K. A., and Benghiat P. (2010). Dyke propagation and sill formation in a compressive tectonic environment. *Journal of Geophysical Research* 115, B08201, <https://doi.org/10.1029/2009JB006791>

Mortimer N., Campbell H.J., Tulloch A.J., King P.R., Stagpoole V.M., Wood R.A., Rattenbury M.S., Sutherland R., Adams C.J., Collot J., and Seton M. (2017). Zealandia: Earth's Hidden Continent. *GSA Today* 27, 3, 27–35 <https://doi.org/10.1130/GSATG321A.1>

Nicolas, A. (1989). *Structure of Ophiolites and Dynamics of Oceanic Lithosphere*. Kluwer, Dordrecht, 367.

Patriat, M., Collot, J., Etienne, S., Poli, S., Clerc, C., Mortimer, N., Pattier, F. and Juan, C. (2018). New Caledonia obducted Peridotite Nappe, offshore extent and implications for obduction and post-obduction processes. *Tectonics*, 37, 1-20, <https://doi.org/10.1002/2017TC004722>

Pirard, C. and Spandler, C. (2017). The zircon record of high-pressure metasedimentary rocks of New Caledonia: Implications for regional tectonics of the south-west Pacific. *Gondwana research*, 46, 79-94, <https://doi.org/10.1016/j.gr.2017.03.001>

Potel S., Ferreiro Mählmann R., Stern V., B. Mullis J. and Frey M. (2006). Very low-grade metamorphic evolution of pelitic rocks under high-pressure/low temperature conditions, NW New Caledonia (SW Pacific). *Journal of Petrology*, 47, 5, 991–1015 <https://doi.org/10.1093/petrology/egic001>

Prinzhofer, A. and Nicolas, A. (1980). The Bogota peninsula, New Caledonia: A possible oceanic transform fault. *Journal of Geology*, 88, 387-398. <https://doi.org/10.1086/628523>

Quesnel B., Gautier P., Boulvais Ph., Cathelineau M., Maurizot P., Cluzel D., Ulrich M., Guillot S., Lesimple S., and Couteau C., (2013). Syn-tectonic, meteoric water-derived carbonation of the New Caledonia Peridotite Nappe. *Geology*, 41 (10), 1063–1066. <https://doi.org/10.1130/G34531.1>

Quesnel, B., Gautier, P., Cathelineau, M., Boulvais, P., Couteau, C. and Drouillet, M. (2016). The internal deformation of the Peridotite Nappe of New Caledonia: a structural study of serpentine-bearing faults and shear zones in the Koniambo Massif. *Journal of Structural Geology*, 85, 51-67, <https://doi.org/10.1016/j.jsg.2016.02.006>

Rawling, T.J. (1998). *Oscillating orogenesis and exhumation of high-pressure rocks in New Caledonia, SW Pacific*. PhD Thesis, Department of Earth Sciences, Monash University, Melbourne Australia.

Schellart W.P., Lister G.S., and Toy V.G. (2006). A Late Cretaceous and Cenozoic reconstruction of the Southwest Pacific region: Tectonics controlled by subduction and slab rollback processes. *Earth-Science Reviews* 76 : 191–233 <https://doi.org/10.1016/j.earscirev.2006.01.002>

Schellart W.P. and Spakman W. (2012). Mantle constraints on the plate tectonic evolution of the Tonga–Kermadec–Hikurangi subduction zone and the South Fiji Basin region. *Australian Journal of Earth Sciences* 59, 6, 933-952. <https://doi.org/10.1080/08120099.2012.679692>

Sécher, D. (1981). Les lherzolites ophiolitiques de Nouvelle-Calédonie et leurs gisements de chromite. Ph D. thesis, Université de Nantes, France, 228.

Sevin B., Ricordel-Prognon C., Quesnel F., Cluzel D., and Maurizot P. (2012). First paleomagnetic dating of ferricrete in New Caledonia: new insight on the morphogenesis and paleoweathering of 'Grande Terre'. *Terra Nova* 24, 77-85. <https://doi.org/10.1111/j.1365-3121.2011.01041.x>

Soret, M., Agard, P., Dubacq, B., Vitale-Brovarone, A., Moiré, P., Chauvet, A., Whitechurch, H., and Villemant, B. (2016). Strain localization and fluid infiltration in the mantle wedge during subduction initiation: Evidence from the base of the New Caledonia ophiolite, *Lithos* 244, 1-19. <https://doi.org/10.1016/j.lithos.2015.11.022>

Spandler, C., Hermann, J., Arculus, R. and Mavrogenes, J.A. (2003). Redistribution of trace elements during prograde metamorphism from lawsonite blueschist to eclogite facies; implications for deep subduction-zone processes. *Contribution to Mineralogy and Petrology*, 146, 205-222. <https://doi.org/10.1007/s00410-003-0195-5>

Spandler, C., Hermann, J., Arculus, R. and Mavrogenes, J. (2004). Geochemical heterogeneity and element mobility in deeply subducted oceanic crust; insights from high-pressure mafic rocks from New Caledonia. *Chemical Geology* 206, 21-42. <https://doi.org/10.1016/j.chemgeo.2004.01.006>

Spandler C., Rubatto D. and Hermann J. (2005). Late Cretaceous-Tertiary tectonics of the southwest Pacific: Insights from U-Pb sensitive, high-resolution ion microprobe (SHRIMP) dating of eclogite facies rocks from New Caledonia. *Tectonics* 24, TC3003, <https://doi.org/10.1029/2004TC001709>

Tarling, D. H. (1967). Results of a paleomagnetic reconnaissance of the New Hebrides and New Caledonia. *Tectonophysics* 4: 55–68. [https://doi.org/10.1016/0040-1951\(67\)90058-3](https://doi.org/10.1016/0040-1951(67)90058-3)

Théveniaut H., Prognon C., and Delor C. (2017). Construction d'une courbe de dérive apparente des poles (CDAP) de Nouvelle Calédonie. Rapport final. BRGM/RP-67339-FR

Teyssier, C., Chatzaras, V. and Von Der Handt, A. (2016). Microfabrics in depleted mantle plaeotransform (New Caledonia). *Geophysical Research Abstracts*, European Geoscience Union, EGU2016-11489, 18.

Titus, S.J., Maes, S.M., Benford, B., Ferre, E.C. and Tikoff, B. (2011). Fabric development in the mantle section of a paleotransform fault and its effect on ophiolite obduction, New Caledonia. *Lithosphere* 3, 221-244, <https://doi.org/10.1130/l122.1>

Uruski C. and Wood R. (1991). A new look at the New Caledonia Basin, an extension of the Taranaki Basin, offshore North Island, New Zealand. *Marine and Petroleum Geology* 8, 4, 379-391. [https://doi.org/10.1016/0264-8172\(91\)90061-5](https://doi.org/10.1016/0264-8172(91)90061-5)

Van de Beuque S. (1999). Evolution géologique du domaine peri-calédonien (sud-ouest Pacifique). PhD thesis Université de Bretagne occidentale, France, 210 pp.

Van de Lagemaat S. H. A., van Hinsbergen D. J. J., Boschman L. M., Kamp P. J. J., and Spakman W. (2018). Southwest Pacific absolute plate kinematic reconstruction reveals major Cenozoic Tonga-Kermadec slab dragging. *Tectonics* 37, 8, 2647–2674. <https://doi.org/10.1029/2017TC004901>

Vitale Brovarone, A., and Agard, P. (2013). True metamorphic isograds or tectonically sliced metamorphic sequence? New high-spatial resolution petrological data for the New Caledonia case study. *Contributions to Mineralogy and Petrology*, 166 (2), 451–469. <https://doi.org/10.1007/s00410-013-0285-2>

Vitale Brovarone A., Agard P., Monié P., Chauvet A., and Rabaute A., (2017). Tectono-metamorphic architecture of the HP belt of New Caledonia. *Earth Science Reviews* 168, 48-67. <https://doi.org/10.1016/j.earscirev.2018.01.006>

Vogt, J. and Podvin, P. (1983). Carte Géologique à l'échelle du 1 / 50 000 et notice explicative: feuille Humboldt-Port-Bouquet. Territoire de Nouvelle-Calédonie - Bureau de Recherches Géologiques et Minières, 1-68.

Wenner, D.B., Taylor, H.P. Jr. (1971). Temperatures of serpentinization of ultramafic rocks based on O^{18}/O^{16} fractionation between coexisting serpentine and magnetite. *Contrib. Mineral. Petrol.* 32, 165-185. <https://doi.org/10.1007/BF00643332>

Whattam, S. A. (2008). Arc-continent collisional orogenesis in the SW Pacific and the nature, source and correlation of emplaced ophiolitic nappe components, *Lithos* 113, 1–2, 88-114. <https://doi.org/10.1016/j.lithos.2008.11.009>

Figure captions

Figure 1: Geological sketch map of New Caledonia restricted to the geological units addressed in this article. Abbreviations in main map: BSZ Belep Shear Zone; BTF Bogota Transform Fault; HC Humboldt Corridor. Inset, color chart; dark red: continental crust, light red: thinned continental crust, light blue: oceanic crust, dark blue: oceanic plateau; abbreviations, LHR : Lord Howe Rise, NR : Norfolk (New Caledonia) Ridge, LR : Loyalty Ridge, HP : Hikurangi Plateau.

Figure 2: Non-sheared coarse-grained diorite dykes and sills crosscutting deeply serpentinised harburgite to exemplify magma injection in an already fractured rock. The dotted lines represent the attitude of the gently dipping mantle fabric of the peridotite. Ore drying area, western bottom of the Tiebaghi Massif (164.20344; -20.48416).

Figure 3: Non-sheared lower Eocene dykes (Massif du Sud), (a) leucogabbro dyke at the confluence of Napouédjeine and Pirogues rivers (166.73031; -22.20831) ; (b) hornblende-gabbro pegmatoid dyke crosscutting a pyroxenite body, Plum Pass (166.68603; -22.30102); (c) detailed view of (b) to show fragmented amphibole crystals coated or 'injected' by plagioclase (lens cap size is 6 cm).

Figure 4: Non-sheared hornblende leucogabbro dyke crosscutting pyroxenite, Plum Pass (166.67156; -22.30200); (b) sheared leucogabbro with c and s shear structures at the walls and transposed c-s mylonitic foliation at the centre (Plum Pass); (166.67233; -22.30285); (c) and (d) detailed views of the central mylonite showing amphibole and orthopyroxene rotated porphyroclasts. All shear indicators are consistent with reverse-sinistral, top-to-the-NW motion.

Figure 5: (a) Internal folds in a layered gabbro dyke of Ouen Island (166.80956; -22.41200); (b) detailed view of the former, showing extremely sharp fold hinges. The white arrow points to an anthophyllite reaction rim around an eroded peridotite xenolith; (c) partly disrupted flow fold structure in a weathered felsic sill, Ouen Island (166.80783; -22.41255); (d) sheared and foliated dyke (yellow arrows) injected by en-echelon leucogabbro lenses (white arrows), the foliated part of the dyke shows sinistral motion (strike N145E), ancient chromite mine Georges Piles (166.75567; -22.24885).

Figure 6: Plot of orientations of lower Eocene dykes and sills from the Peridotite Nappe at island scale (Schmidt equiaerial stereonet, lower hemisphere). Bold circles represent sheared dykes (with sense of shear).

Figure 7: (a) Dolerite lensoids within a serpentinised normal fault (Kopeto Massif); (b) detailed view of the fault zone to show the c-s structure with down-dip motion.

Figure 8: (a) Antigorite crack seal on a small dextral fault (offset < 10 cm); (b) tremolite-bearing crack seal (photo credit: Lahondère, 2012).

Figure 9: (a) Plot and kinematic analysis of antigorite and tremolite-antigorite-bearing small faults (main axes of the strain ellipsoid: X= stretching, Y intermediate, Z shortening). Note that the majority of mineral fibers indicate strike slip or oblique slip motion. The insert (b) illustrates the permutation of the main strain axes (X/Y and Y/Z). The strain ellipsoid axes have been computed with the FaultKin application (Allmendinger et al., 2012), (Schmidt equal-area stereonet, lower hemisphere).

Figure 10: A typical outcrop of Poya Terrane Basalts to show tectonically interleaved upright basalt (bas) and abyssal argillite (arg) slices, the whole set was sheared toward the SW and developed some schistosity beneath the Peridotite Nappe (CF 34 track); (165.27649; -21.47172).

Figure 11: Tectonic map of the Poya Terrane to show the regional-scale “Z” type folds with vertical axes consistent with dextral transpression. It is worth to note that PTB and KF display the same large-scale structure while the underlying autochthonous/parautochthonous units display a much simpler organization (blue line).

Figure 12: Formation and structure of the Poya Terrane in a three-step model of intra-oceanic accretion and oblique subduction. KF: Kone Facies (turbidites); PTB: Poya Terrane Basalts. Blue: oceanic crust, green: upper mantle peridotites, orange: continental crust.

Figure 13: (a) Tectonic map of the Eocene HP-LT belt of northern New Caledonia. The blue lines show the orientation of regional structures (foliation, bedding, serpentinite or melange slices). Bold black lines represent the trend of structures when they can be traced over long distances (> 20 km). Large-scale “Z” type folds appear in high-grade part of the metamorphic domain. It is worth to note the southwestward decrease of the folds closure and southeastward changing style from open fold into fault-fold. (b) cartoon showing the relationship of “Z” type folds and regional-scale transpression. (c) structural map of the restored orientation of the stretching lineation.

Figure 14: Equal-area projection of directions from Characteristic Remanence Magnetization (ChRM). a. directions in-situ coordinates; b. directions in bedding corrected coordinates.

Figure 15: Paleomagnetic poles from this study and Dallanave et al. (2020) with the Australian APWP (Besse and Courtillot, 2002, 2003)

Figure 16: Attempted paleogeographic reconstruction of the Southwest Pacific during the Eocene to account for: (a) lower Eocene subduction inception at or near a RRR triple junction, (b) oblique pre-obduction subduction; (c) subduction jamming by the Norfolk Ridge and counterclockwise rotation of New Caledonia; and (d) final blocking of the subduction in New Caledonia by the Lord Howe Rise; meanwhile, the subduction continued to the south (modified from Cluzel et al., 2001, 2012a; Meffre et al., 2006; Patriat et al., 2018). (NC: New Caledonia, NR: Norfolk Ridge, LHR: Lord Howe Rise, NLB: North Loyalty Basin, AUSTR: Australia, V: Vanuatu, T: Tonga, K: Kermadec, gray bold line: active spreading ridge, dark blue bold line: extinct spreading ridge.

Table 1: Paleomagnetic results from southern New Caledonia. n/N , D , I , α , g and s stand for statistic/total measured samples, declination, inclination cone radius α of statistic confidence at 95%, in-situ, bedding-corrected coordinates, respectively.

Table 2: Comparison of paleomagnetic results from New Caledonia with Australian APWP. λ and ϕ stand for latitude and longitude of paleomagnetic pole respectively; d_p , d_m and A_{95} stand for statistic errors in latitude and rotation at 95% confidence level. Australian poles are from Besse and Courtillot (2002, 2003). Differences are calculated at 21.8°N , 165.9°E (average of geographic coordinates of sites A, B, E, F). Error bars are calculated by $(0.63^*) \text{root}(A_{95}^2 + D_p \text{ or } m^2)$ (Demarest, 1983).

Table 3: Summary of tectonic features deduced from the structural analysis of the Poya Terrane, Peridotite Nappe and Eocene metamorphic belt. All kinematic axes have been computed in the present orientation of the island and do not account for $\sim 60^\circ$ counterclockwise rotation.

Site	location	Formation	Lithology	Age	n/N	Sampling coordinates		Paleomagnetic direction				
						Lat. (°N)	Long. (°E)	Dg (°)	Ig (°)	α_{95g} (°)	Ds (°)	Is (°)
A	Gadji Bay (Dumbea)	Bourail Flysch	siltstone	~35	6/11	-22.20	166.35	338.7	-44.5	19.6	358.8	-33
E	Nessadiou, RT1, Cimetièrè des Arabes	Bourail Flysch	Fine grained sandstone	~35	4/6	-21.62	165.55	355.7	-8.3	25.2	349.6	-38
F	Roche Percée, Bourail	Priabonian Bourail Flysch	siltstone	~35	4/7	-21.61	165.46	326.9	-34.4	23.9	322.2	-37
G	Col Aymes	Lutetian Bourail Flysch	Calcareous sandstone	~42	0/4	-21.67	165.55	No stable ChRM isolable				
H	Tontouta River	lower Eocene	Dolerite	~50	0/7	-21.92	166.33	No stable ChRM isolable				
AEF				~35	14/1	-21.90	165.95	341.1	-31.8	14.0	345.9	-36

Table 1. Paleomagnetic results from southern New Caledonia

n/N, D, I, α , g and s stand for statistic/total measured samples, declination, inclination cone radius of statistic confidence at 95%, in-situ, bedding-corrected coordinates, respectively.

Au niveau des sites, les statistiques sont moins bonnes après corrections de pendage par rapport avant corrections, mais les moyennes en âge change la tone.

Journal Pre-proof

Age	New Caledonia Pole				Australian Pole			Difference in latitude (°)	Difference in rotation (°)	Refer
	λ	ϕ	dp (°)	dm	λ	ϕ (°)	A ₉₅			
35 Ma	76.8	79.7	8.5	14.6	72.9	285.3	4.5	-8.9 ± 6.1	-31.2 ± 9.6	This s
45Ma	50.5	29.0	4.2	5.3	70.2	294.6	5.4	11.7 ± 4.3	-56.2 ± 4.8	Dallan al., 2

Table 2. Comparison of paleomagnetic results from New Caledonia with Australian APWP

λ and ϕ stand for latitude and longitude of paleomagnetic pole, respectively; dp, dm and A₉₅ stand for statistic

errors in latitude and rotation at 95% confidence level. Australian poles are from Besse and Courtillot (2002, 2003).

Differences are calculated at -21.8°N, 165.9°E (average of geographic coordinates of sites A, B, E, F).

Error bars are calculated by $(0.63^*) \text{ root } (A_{95}^2 + D_p \text{ or } d_m^2)$ (Demarest, 1983).

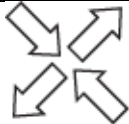
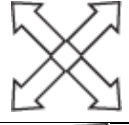
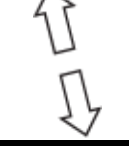
Unit	Tectonic feature	Events	Timing	Main strain axes
Metamorphic sole	Granulite facies amphibolites	Subduction inception (ironing effect)	> 56 Ma	?
Intermediate Mélange	Andesitic pillow lavas-diorites Supra-subduction dykes	Fore-arc basin Slab melting Mantle wedge re-melting	54.5 - 54 Ma	?
Pouébo Mélange	melanged supra-subduction dykes	Slab melting	55.5 – 55 Ma	?
Peridotite Nappe	supra-subduction dykes	Sheared dykes (Slab melting)	55.5 - 55 Ma	
	supra-subduction dykes	Non-sheared dykes (Slab melting mantle wedge re-melting)	55 - 50 Ma	
	IAT dolerites	Latest fore-arc magmatism	>50 - 47 Ma	 or
	Antigorite-tremolite and antigorite crack seals	Heat/pressure solution Metasomatism by slab fluids	54? - ? Ma	
Poya Terrane Basalts	Sliced upper oceanic crust	Fore-arc accretion	56 – 45 Ma	?
Koné Facies	Distal turbidites	Passive margin	85 – 70 Ma	–
Poya Terrane (PTB + KF)	Melange allochthon	“Z” type folds	~ 45 Ma	
Bourail Flysch	Eocene foreland basin	South- or south-eastward propagating	45 – 35 Ma	?
HP-LT Diahot-Panié and Pouébo terranes	Subduction complex	exhumation	44 – 34 Ma	
		“Z” type folds	> 34 Ma	
Peridotite Nappe	Serpentinite sole	obduction	? - < 34 Ma	

Table 2: Summary of tectonic features deduced from the structural analysis of the Poya Terrane, Peridotite Nappe and Eocene metamorphic belt. All kinematic axes have been computed in the present orientation of the island and do not account for counterclockwise rotation.

Journal Pre-proof

Highlights

- The structural analysis of the Eocene subduction-obduction complex of New Caledonia reveals a polyphase evolution
- Paleomagnetic data from autochthonous terranes record *ca* 56° counterclockwise rotation during the mid- to late Eocene
- The upper plate represented by the ultramafic fore-arc allochthon underwent oblique-slip dominated dilatational tectonics associated with northward subduction in rapidly cooling conditions
- The allochthonous Poya Terrane and metamorphic units of the HP-LT belt display Z-type folds due to dextral shearing prior to final tectonic emplacement
- Finally, ultramafic rocks were obducted with top-to-the-SW kinematics

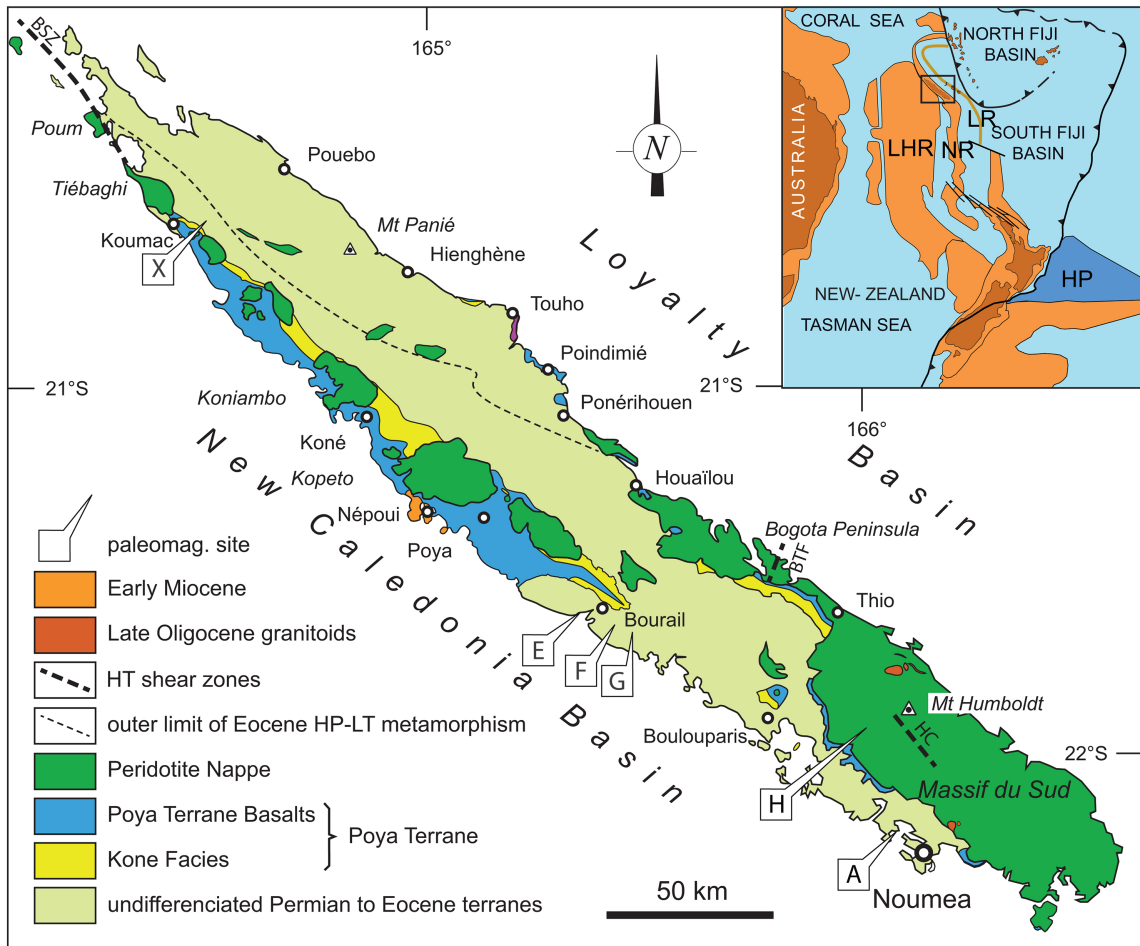


Figure 1

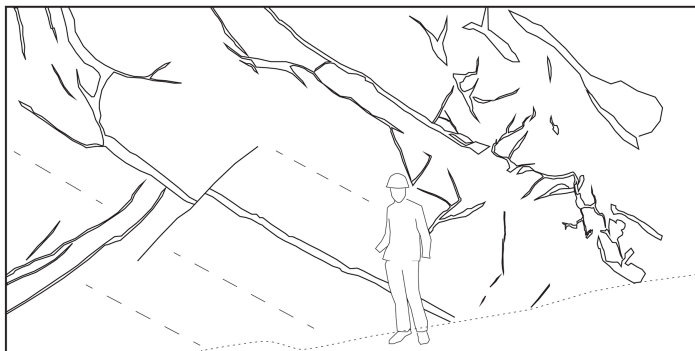


Figure 2



Figure 3

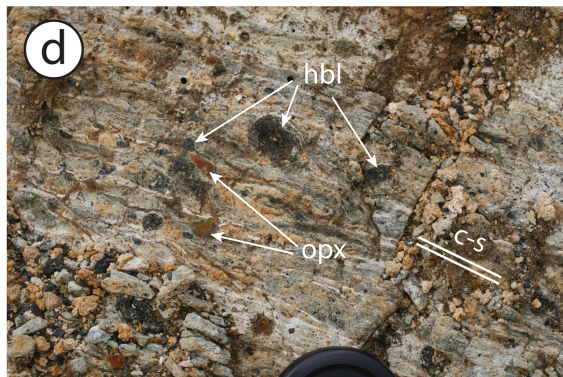
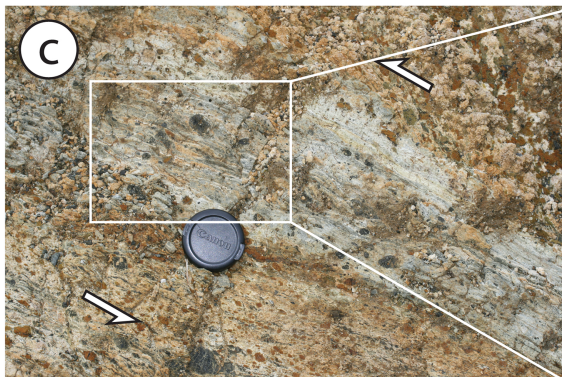
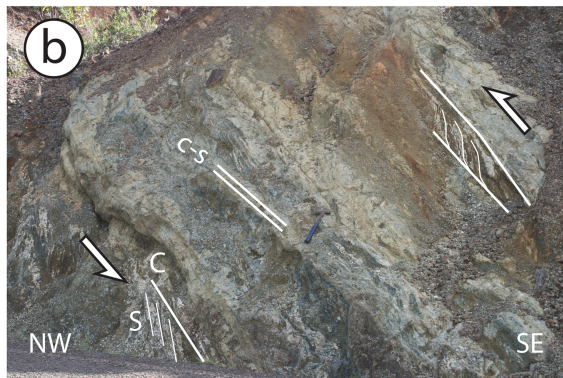


Figure 4

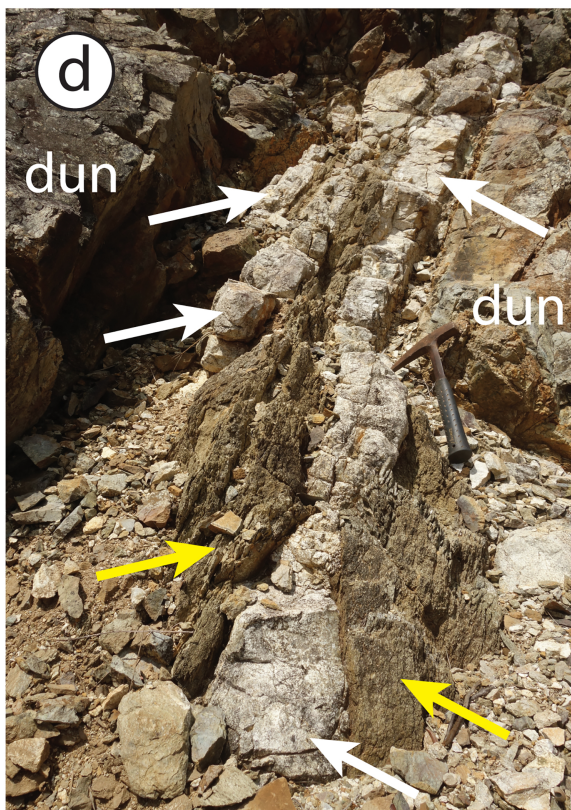
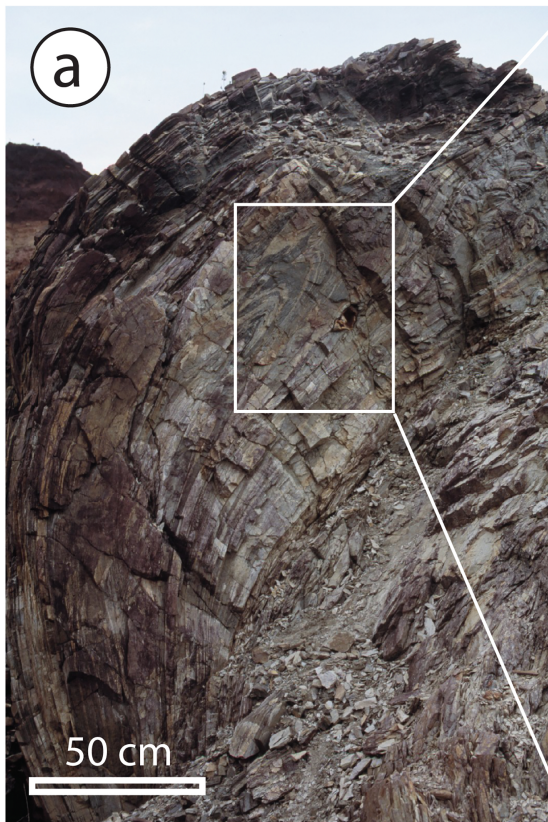


Figure 5

Lower Eocene dykes and sills

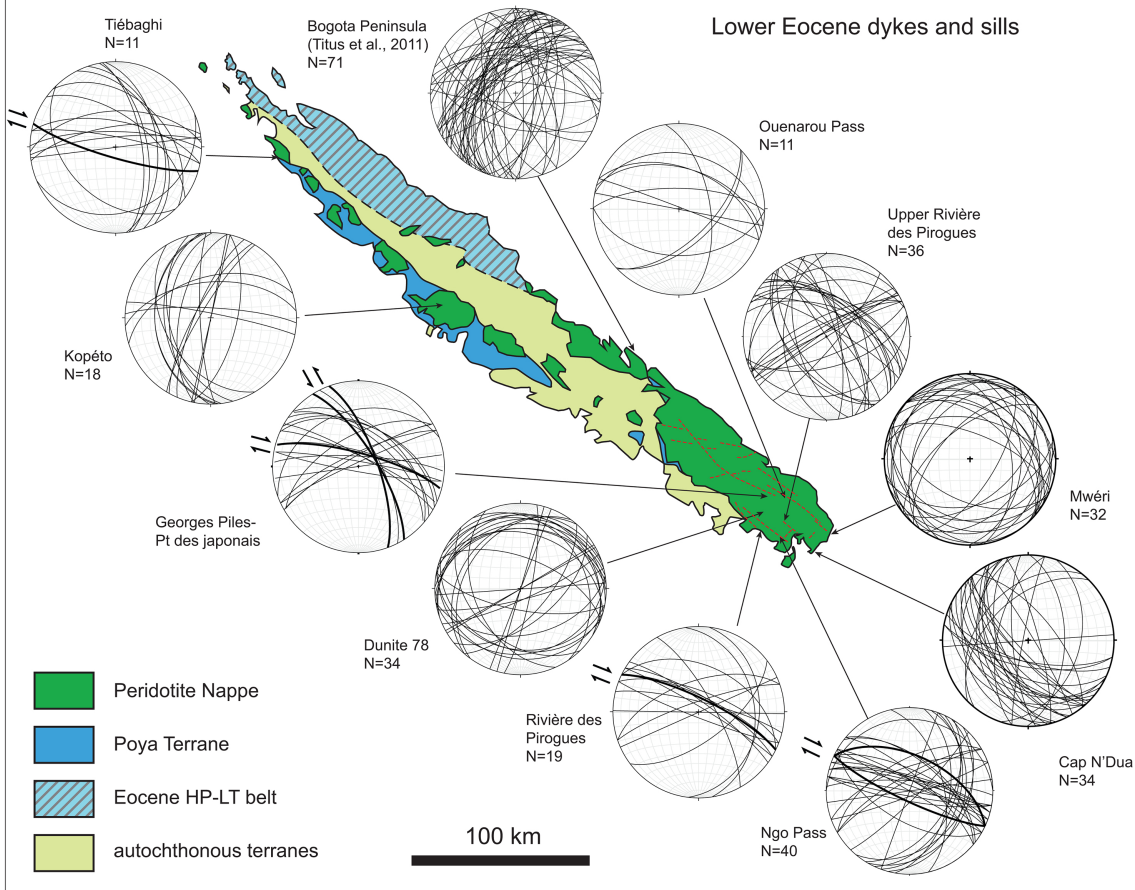


Figure 6

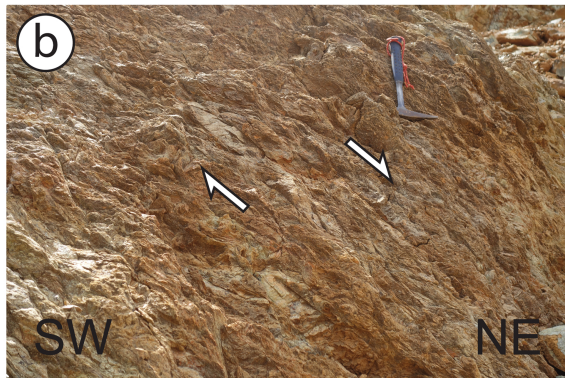
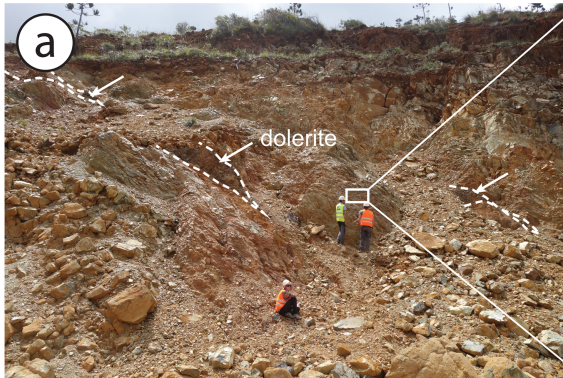


Figure 7



Figure 8

(a) Antigorite/tremolite-bearing tension and shear cracks

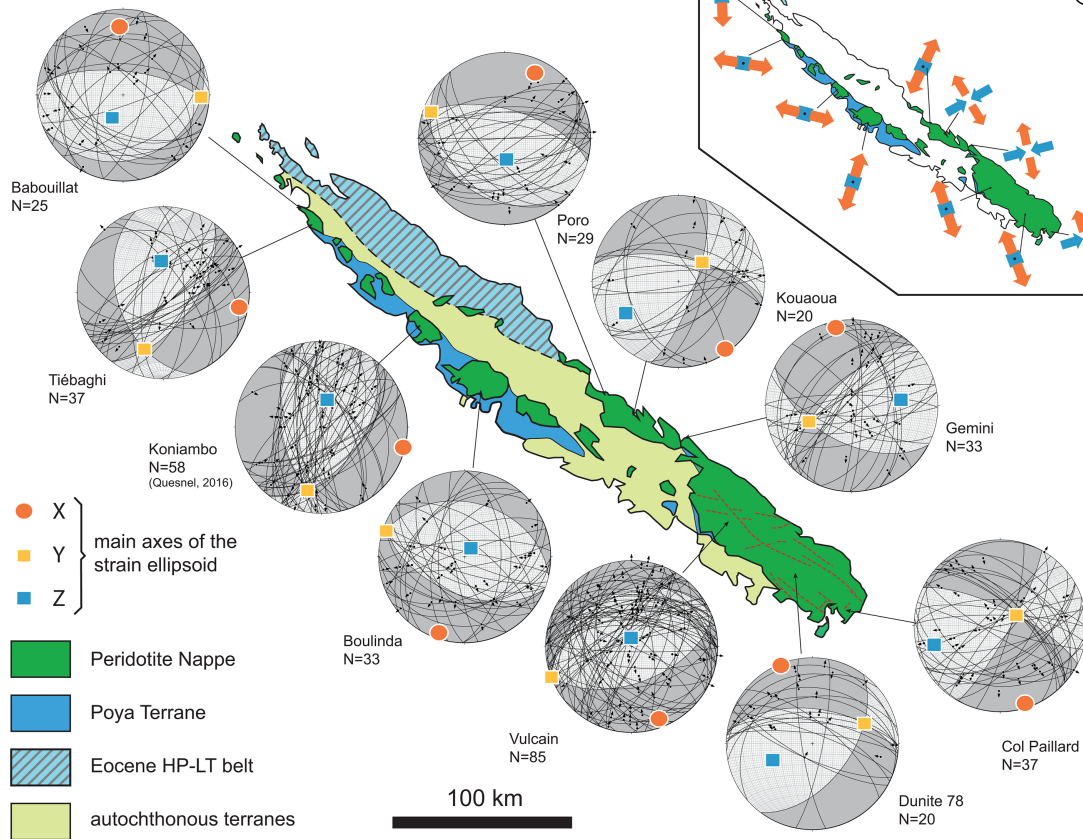


Figure 9

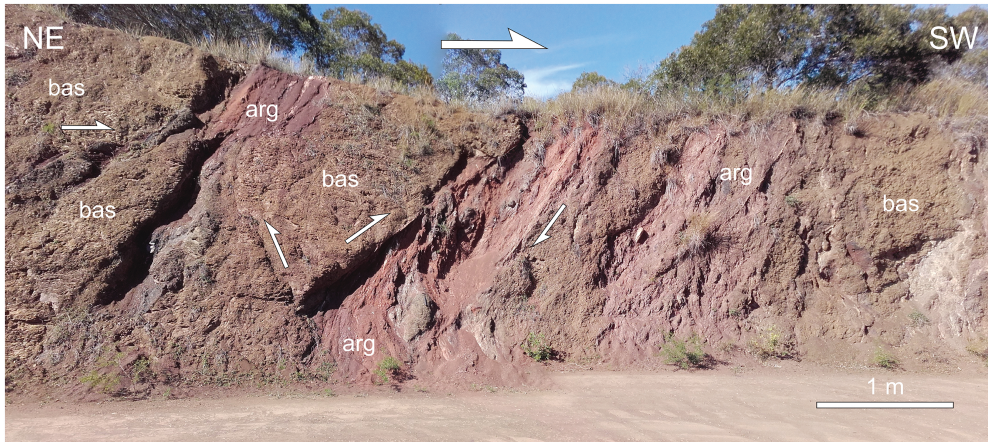


Figure 10

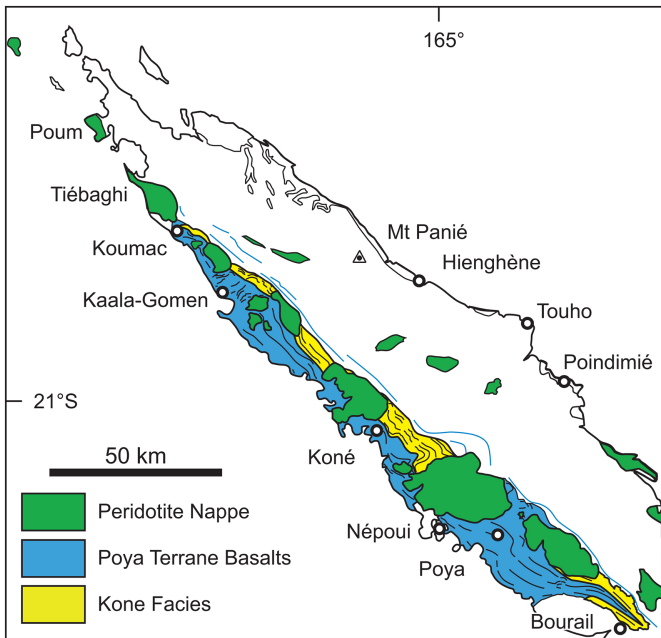


Figure 11

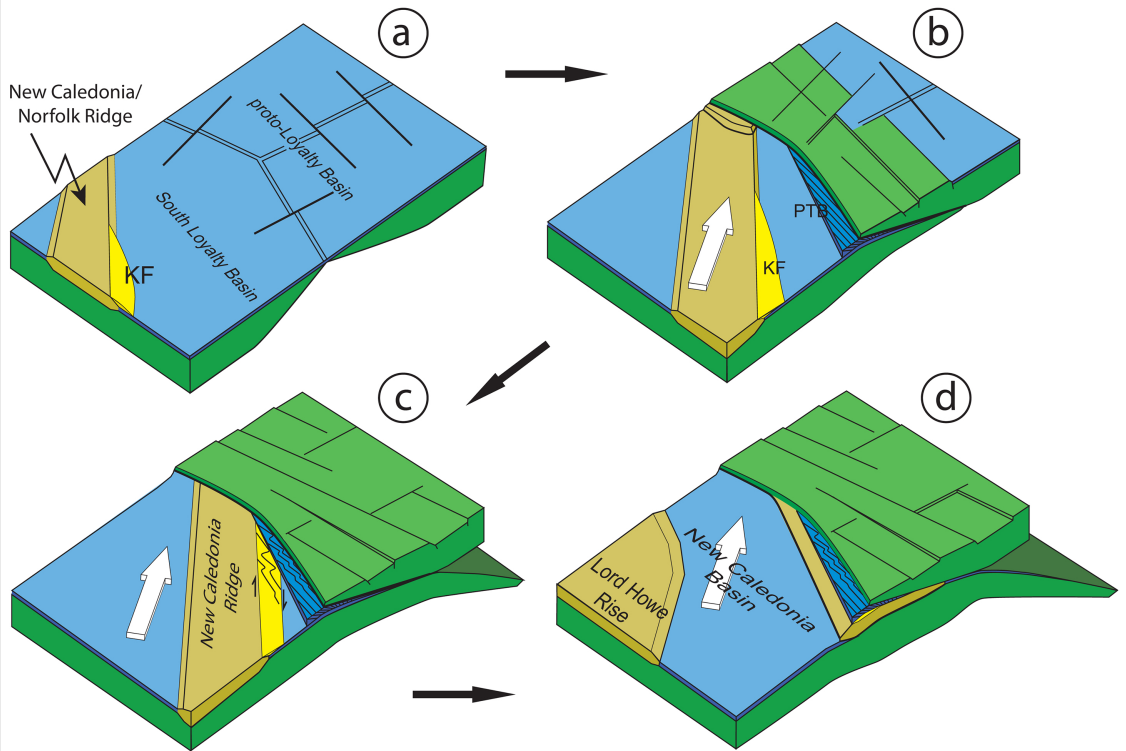


Figure 12

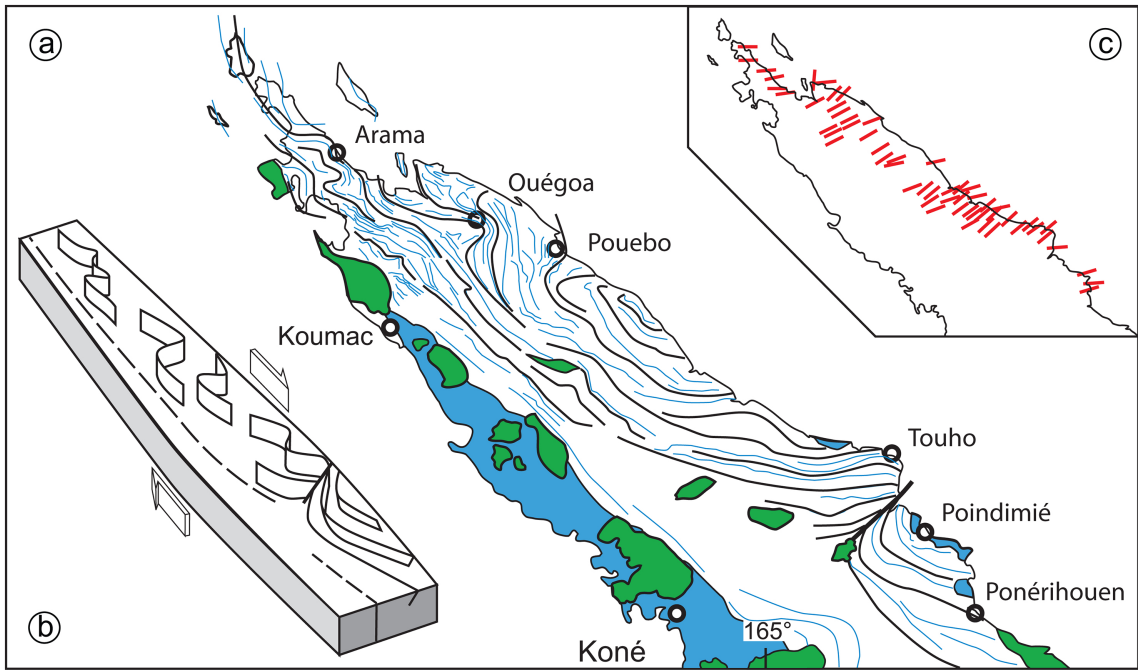
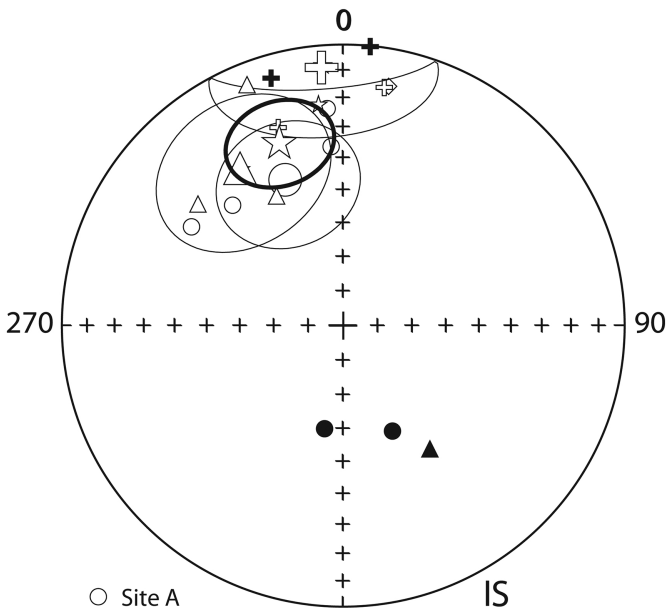


Figure 13



○ Site A

⊕ Site E

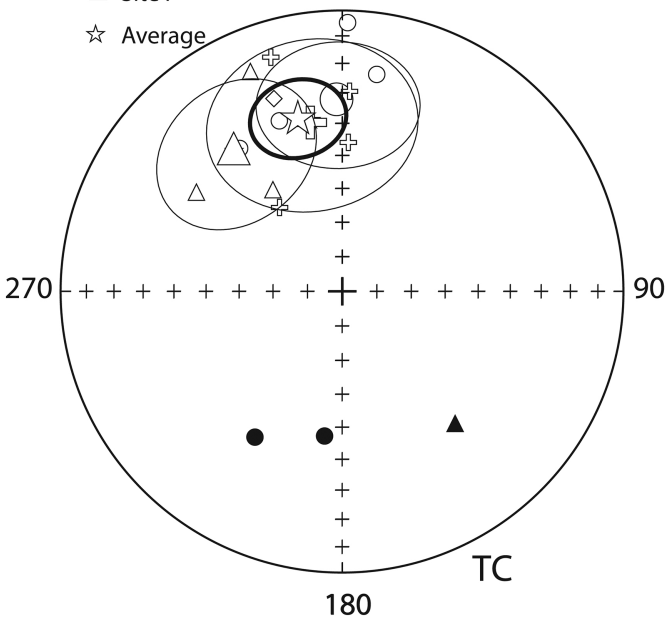
△ Site F

☆ Average

IS

180

0



TC

180

Figure 14

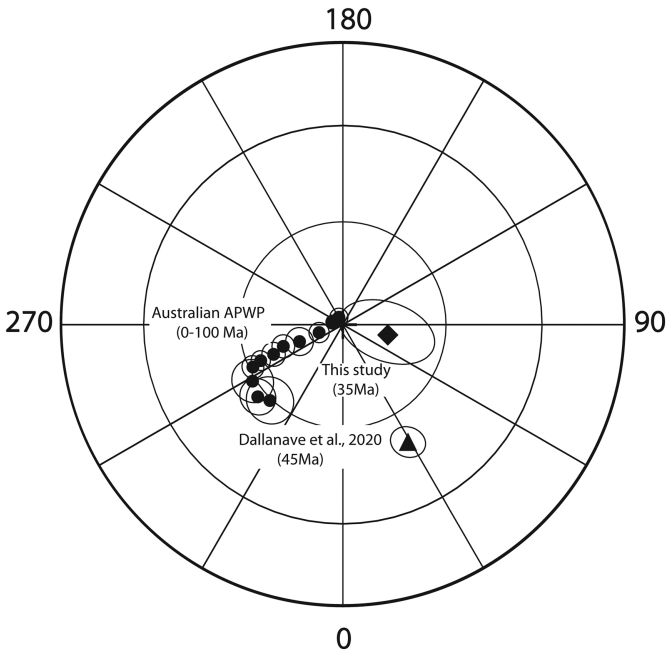


Figure 15

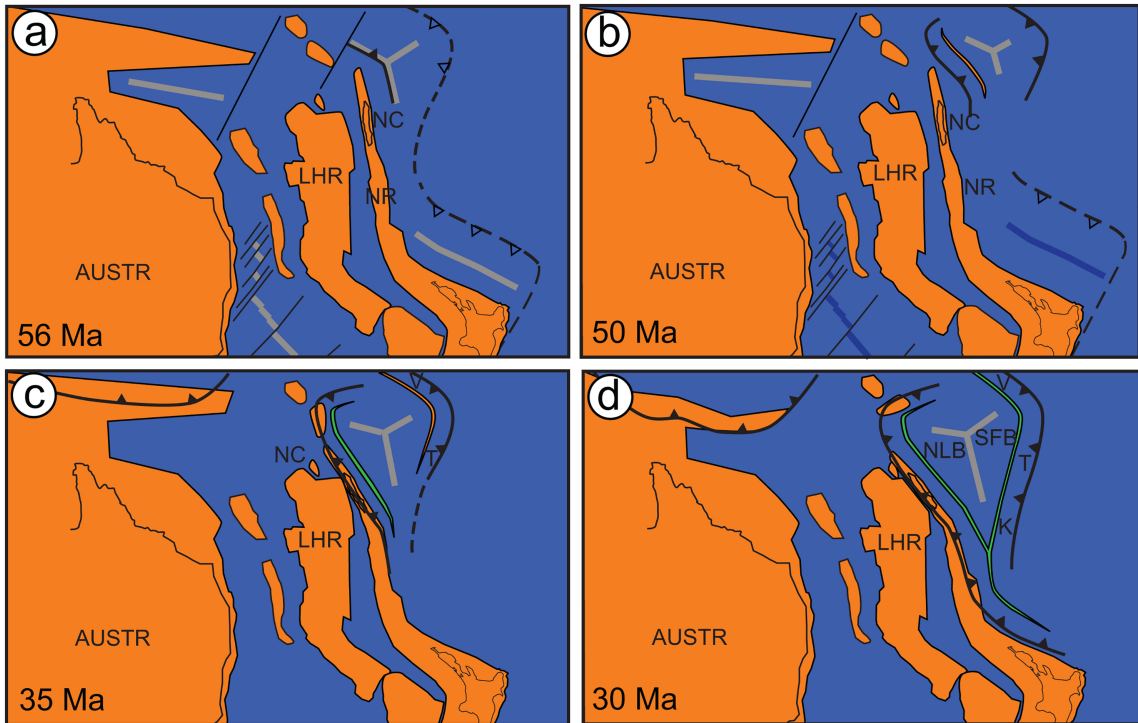


Figure 16